Reactions of η^2-Acyl Ligands in $Tp'(CO)_2Mo[\eta^2\text{-}C(O)R]$ Complexes To Form Complexed Enolates and Enones, Allyls, and Alkyne Insertion Products

C. A. Rusik, M. A. Collins, A. S. Gamble, T. L. Tonker, and J. L. Templeton*

Contribution from the W. R. Kenan, Jr. Laboratory, Department of Chemistry, University of North Carolina, Chapel Hill, North Carolina 27599. *Received September 12, 1988*

Abstract: Elaboration of the η^2-acyl ligand in hydridotris(3,5-dimethylpyrazolyl)borate (Tp′) complexes of the type $Tp'(CO)_2Mo[\eta^2\text{-}C(O)R]$ (R = Me, Et) has been accomplished by deprotonation to form enolates which react with electrophiles such as MeI, $PhCH_2Br$, and PhCHO. Two enolate complexes, $K[Tp'(CO)_2Mo(C(O){=}CH_2)]$ and $K[Tp'(CO)(P(OPh)_3)MoC(O){=}CHMe]$, have been characterized by NMR spectroscopy. Photolysis of an acetonitrile solution of the achiral dicarbonyl reagent, $Tp'(CO)_2Mo[\eta^2\text{-}C(O)R]$, followed by addition of triphenyl phosphite forms racemic $Tp'(CO)[P(OPh)_3]Mo[C(O)R]$. Excellent diastereoselectivity characterizes the addition of benzyl bromide (BzBr) to the enolate of $Tp'(CO)[P(OPh)_3]Mo[\eta^2\text{-}C(O)CH_2CH_3]$; the $Tp'(CO)[P(OPh)_3]Mo(\eta^2\text{-}C(O)CHMeBz)$ product has been structurally characterized. Condensation of enolate complexes with benzaldehyde or benzophenone produces unsaturated η^2-enone complexes. The structure of $Tp'(CO)_2Mo[\eta^2\text{-}C(O)CH{=}CPh_2]$ is reported. The η^2-enone complexes undergo conjugate addition reactions to form saturated η^2-acyl products, e.g., nucleophilic addition of MeLi to $Tp'(CO)_2Mo(\eta^2\text{-}C(O)CH{=}CHPh)$ followed by acidification yields $Tp'(CO)_2Mo[\eta^2\text{-}C(O)CH_2CHMePh]$. Heating $Tp'(CO)_2Mo(\eta^2\text{-}C(O)CMe{=}CHPh)$ in toluene yields a π-allyl complex, $Tp'(CO)_2Mo(\eta^3\text{-}CH_2CHCHPh)$. Insertion of alkynes (RC≡CR, R = Et or Ph) into the metal–carbon bond of the η^2-acyl ligand in $Tp'(CO)(CH_3CN)Mo(\eta^2\text{-}C(O)Et)$ under carbon monoxide forms oxametallacycles of the type $Tp'(CO)_2Mo(CRCRC(O)Et)$ (R = Et or Ph). The structure of $Tp'(CO)_2Mo(CEtCEt(O)Et)$ has been determined.

Chiral enolates are an important class of reagents.[1] Excellent diastereoselectivity has been achieved with chiral organic auxiliaries,[2] and transition-metal centers can also act as chiral adjuvants in enolate reactions. Stereoselective reactions of iron enolate species derived from $[(\pi\text{-}C_5H_5)(PPh_3)(CO)FeC(O)CH_2R]$ have been studied extensively.[3,4] The utility of the chiral $[(\pi\text{-}C_5H_5)(NO)(PPh_3)Re]$ moiety has been demonstrated,[5] and cobalt enolate reagents have been prepared from cyclic acyl complexes.[6]

Early examples of transition-metal η^2-acyl complexes were dominated by d^0 group IV elements[7] or other oxophilic metals,[8] but a number of group VI η^2-acyl complexes are now known.[9,10] The chemistry accessible from molybdenum η^2-acyl reagents has not yet been defined.

This paper reports representative chemistry of enolate reagents generated by deprotonation of η^2-acyl precursors of the form $Tp'(CO)(L)MoC(O)R$ (Tp′ = hydridotris(3,5-dimethylpyrazolyl)borate).[11,12] The sterically demanding Tp′ ligand[13] should be more effective in directing approach to the enolate moiety than cyclopentadienyl species studied to date, and cyclopentadienyl ligands are susceptible to deprotonation under strongly basic conditions.[14] Furthermore, Tp′ complexes tend to be more resistant to aerial oxidation than their cyclopentadienyl analogues. It seems reasonable to expect that deprotonation of an η^2-acyl ligand will yield a more rigid enolate species and thus afford better stereocontrol in subsequent reactions than related η^1-acyl reagents. The role of molybdenum as an internal Lewis acid binding the acyl oxygen should strongly influence enolate chemistry both kinetically and thermodynamically.

Preparations of η^2-acyl complexes, spectroscopic characterization of enolate reagents, alkylation reactions, and aldol condensations to form η^2-enone elimination products are reported here; representative results have been communicated previously.[15] Conjugate additions to η^2-enone ligands and thermal rearrangement of an α-methyl enone complex to form a π-allyl product are now reported. Alkyne addition to an η^2-acyl complex with a labile acetonitrile ligand gives insertion of the alkyne into the molybdenum–carbon bond of the η^2-acyl to form a metallacyclic product.

Results and Discussion

η^2-Acyl Complexes. η^2-Acyl complexes $Tp'(CO)_2MoC(O)R$ (R = Me, Et) were prepared by a modification of the route used

(1) For a thorough discussion of enolate chemistry, see: *Asymmetric Synthesis*; Morrison, J. D., Ed.; Academic Press: Orlando, FL, 1984; Vol. 3.

(2) (a) Heathcock, C. H. *Asymmetric Reactions and Processes in Chemistry*: Eliel, E. L., Otsuka, S. Eds.; American Chemical Society: Washington, D. C., 1982. (b) Evans, D. A.; Nelson, J. V.; Taber, T. R. *Topics in Stereochemistry*; Allinger, N. L., Eliel, E. L., Wilen, S. H., Eds.; Wiley: New York, 1982; Vol. 13, p 1. (c) Evans, D. A.; Britton, T. C.; Dorow, R. L.; Dellaria, J. F. *J. Am. Chem. Soc.* **1986**, *108*, 6395. (d) Trimble, L. A.; Vederas, J. C. *J. Am. Chem. Soc.* **1986**, *108*, 6397.

(3) Liebeskind, L. S., Welker, M. E.; Fengl, R. W. *J. Am. Chem. Soc.* **1986**, *108*, 6328.

(4) (a) Davies, S. G.; Walker, J. C. *J. Chem. Soc., Chem. Commun.* **1985**, 209. (b) Davies, S. G.; Easton, R. J. C.; Walker, J. C.; Warner, P. *J. Organomet. Chem.* **1985**, 296, C40. (c) Ambler, P. W.; Davies, S. G. *Tetrahedron Lett.* **1985**, *26*, 2129.

(5) (a) O'Connor, E. J.; Kobayashi, M.; Floss, H. G.; Gladysz, J. A. *J. Am. Chem. Soc.* **1987**, *109*, 4837. (b) Bodnar, G. S.; Smith, D. E.; Hatton, W. G.; Heah, P. C.; Georgiou, S.; Rheingold, A. L.; Geib, S. J.; Hutchinson, J. P.; Gladysz, J. A. *J. Am. Chem. Soc.* **1987**, *109*, 7688.

(6) Theopold, K. H.; Becker, P. N.; Bergman, R. G. *J. Am. Chem. Soc.* **1982**, *104*, 5250.

(7) (a) Fachinetti, G.; Fochi, G.; Floriani, C. *J. Chem. Soc., Dalton Trans.* **1977**, 1946. (b) Erker, G. *Acc. Chem. Res.* **1984**, *17*, 103. (c) Wolczanski, P. T.; Bercaw, J. E. *Acc. Chem. Res.* **1980**, *13*, 121. (d) Jeffery, J.; Lappert, M. F.; Luong-Thi, N. T.; Webb, M. *J. Chem. Soc., Dalton Trans.* **1981**, 1593. (e) Baldwin, J. C.; Keder, N. L.; Strouse, C. E.; Kaska, W. C. *Z. Naturforsch.* **1980**, *35b*, 1289. (f) Klei, E.; Teuben, J. H. *J. Organomet. Chem.* **1981**, *222*, 79. (g) Calderazzo, F. *Angew. Chem., Int. Ed. Engl.* **1977**, *16*, 299. (h) Hofmann, P.; Stauffert, P.; Tatsumi, K.; Nakamura, A.; Hoffmann, R. *Organometallics* **1985**, *4*, 404.

(8) (a) Moloy, K. G.; Marks, T. J. *J. Am. Chem. Soc.* **1984**, *106*, 7051. (b) Fagan, P. J.; Manriquez, J. M.; Marks, T. J.; Day, V. W.; Vollmer, S. H.; Day, C. S. *J. Am. Chem. Soc.* **1980**, *102*, 5393. (c) Tatsumi, K.; Nakamura, A.; Hofmann, P.; Stauffert, P.; Hoffmann, R. *J. Am. Chem. Soc.* **1985**, *107*, 4440. (d) For a recent review of η^2-acyl chemistry see: Durfee, L. D.; Rothwell, I. P. *Chem. Rev.* **1988**, *88*, 1059.

(9) (a) Carmona, E.; Sanchez, L.; Marin, J. M.; Poveda, M. L.; Atwood, J. L.; Priester, R. D.; Rogers, R. D. *J. Am. Chem. Soc.* **1984**, *106*, 3214. (b) Bonnesen, P. V.; Yau, P. K. L.; Hersh, W. H. *Organometallics* **1987**, *6*, 1587.

(10) (a) Carmona, E.; Marin, J. M.; Poveda, M. L.; Sanchez, L.; Rogers, R. D.; Atwood, J. L. *J. Chem. Soc., Dalton Trans.* **1983**, 1003. (b) Carmona, E.; Wilkinson, G.; Atwood, J. L.; Rogers, R. D.; Hunter, W. E.; Zarawotko, M. J. *J. Chem. Soc., Dalton Trans.* **1980**, 229. (c) Carmona, E.; Munoz, M. A.; Rogers, R. D. *Inorg. Chem.* **1988**, *27*, 1598.

(11) (a) Trofimenko, S. *J. Am. Chem. Soc.* **1969**, *91*, 588. (b) Curtis, M. D.; Shiu, K.-B.; Butler, W. M. *Organometallics* **1983**, *2*, 1475.

(12) Curtis, M. D.; Shiu, K.-B.; Butler, W. M. *J. Am. Chem. Soc.* **1986**, *108*, 1550.

(13) (a) Trofimenko, S. *Prog. Inorg. Chem.* **1986**, *34*, 115. (b) Trofimenko, S.; Calabrese, J. C.; Thompson, J. S. *Inorg. Chem.* **1987**, *26*, 1507. (c) Calabrese, J. C.; Trofimenko, S.; Thompson, J. S. *J. Chem. Soc., Chem. Commun.* **1986**, 1122.

(14) Heah, P. C.; Patton, A. T.; Gladysz, J. A. *J. Am. Chem. Soc.* **1986**, *108*, 1185.

(15) Rusik, C. A.; Tonker, T. L.; Templeton, J. L. *J. Am. Chem. Soc.* **1986**, *108*, 4652.

0002-7863/89/1511-2550$01.50/0

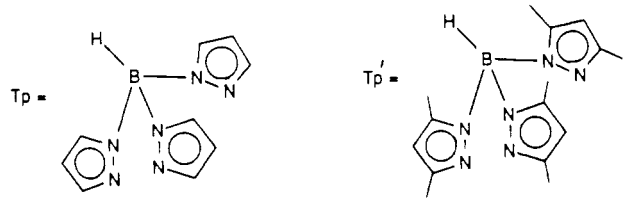

by Trofimenko[11] and Curtis[12] for analogous compounds containing the less hindered Tp ligand (Tp = hydridotris(pyrazolyl)borate). Following generation of $K[Tp'Mo(CO)_3]$ (**1**) in tetrahydrofuran (eq 1),[16] addition of excess alkyl iodide and continued heating affords methyl (**2a**) and ethyl (**2b**) η^2-acyl complexes (Scheme I).

Scheme I

$$KTp' + Mo(CO)_6 \xrightarrow[\Delta \sim 20\ h]{THF} \underset{\mathbf{1}}{K[Tp'Mo(CO)_3]} + 3CO(g) \quad (1)$$

$$K[Tp'Mo(CO)_3] + RI \xrightarrow[\Delta \sim 20\ h]{THF} Tp'(CO)_2Mo[\eta^2\text{-}C(O)R] + KI \quad (2)$$

R = Me, **2a**
R = Et, **2b**

Filtration through alumina yields the pure dicarbonyl η^2-acyl complexes as orange powders which can be briefly handled in air. IR spectra of these neutral compounds exhibit diagnostic Tp' absorbances near 2520 and 1540 cm^{-1}. The η^2-acyl CO stretch was not identified; it may be obscured by the Tp' absorption near 1540 cm^{-1}. The two ν(CO) absorptions are near 1960 and 1830 cm^{-1}; the lower energy band is significantly more intense.

Both ^1H and ^{13}C NMR spectra of η^2-acyl complexes **2a** and **2b** exhibit 2:1 patterns for the dimethylpyrazole signals, indicating that the dmpz rings trans to the carbonyl ligands are equivalent on the NMR time scale. The carbonyl carbon of the acyl ligand appears near 253 ppm; its identity is confirmed by long-range coupling to the protons on C_α ($^2J_{CH}$ = 5–6 Hz). The two metal carbonyl carbons resonate at 233 ppm. In $Tp(CO)_2Mo[C(O)Me]$ the carbonyl ligands are nonequivalent in the solid state[12] but appear as a singlet in the solution ^{13}C NMR spectrum. Curtis has suggested that a low-energy metal–ligand deformation coupled with acyl rotation equilibrates the carbonyl carbons on the NMR time scale.[12] We assume a similar process occurs with the Tp' complexes **2a** and **2b**.

Preparation of phosphite-containing η^2-acyl complexes, $Tp'(CO)(L)MoC(O)R$ [L = $P(OPh)_3$, $P(OMe)_3$, or $P(OEt)_3$], involves photolytic generation of an acetonitrile adduct which reacts with phosphite in a nondonor solvent to form the substituted product (Scheme II).

Scheme II

$$\underset{\mathbf{2a,\ 2b}}{Tp'(CO)_2Mo[\eta^2\text{-}C(O)R]} \xrightarrow[0\ °C]{h\nu,\ CH_3CN} \underset{\mathbf{3a,\ 3b}}{Tp'(CO)(CH_3CN)Mo[\eta^2\text{-}C(O)R]} \quad (3)$$

$$Tp'(CO)(CH_3CN)Mo[\eta^2\text{-}C(O)R] \xrightarrow[30\ min]{L,\ CH_2Cl_2} Tp'(CO)(L)Mo[\eta^2\text{-}C(O)R] \quad (4)$$

4a: L = $P(OPh)_3$, R = Me
4b: L = $P(OPh)_3$, R = Et
5: L = $P(OMe)_3$, R = Et
6: L = $P(OEt)_3$, R = Et

During photolysis the two νCO bands of the starting material are gradually replaced by a single band at 1775 cm^{-1} which is attributed to $Tp'(CO)(CH_3CN)MoC(O)R$ (**3**). This species gradually degrades in solution. Attempts at complete photoconversion to **3** result in diminished yields; about 80% conversion gave the best results. Treatment of **3** with $P(OR)_3$ in CH_2Cl_2 leads to substitution of CH_3CN in about 30 min, as monitored by the growth of an IR peak near 1800 cm^{-1}.

Table I. Approximate Rates of Phosphite Exchange

$Tp'(CO)(L)MoC(O)Et + L' \rightarrow Tp'(CO)(L')MoC(O)Et + L$
4b: L = $P(OPh)_3$
6: L = $P(OEt)_3$

time (h)	[6]/{[4b] + [6]}	time (h)	[4b]/{[6] + [4b]}
1.0	0	1.0	0
2.0	0	2.0	0
24	0.06	24	0
48	0.11	48	0
168	0.44	168	0.04
336	0.71	336	0.05
720	0.82	720	0.06
1848	0.95	1848	0.08

Replacement of CO with $P(OR)_3$ removes the effective mirror symmetry observed on the NMR time scale for the dicarbonyl complexes and renders the three dmpz rings nonequivalent. The metal carbonyl carbon and the acyl carbon appear as ^{31}P coupled doublets near δ 235 ($^2J_{CP} \sim 50$ Hz) and 265 ($^2J_{CP}$ = 14 Hz), respectively.

Significant decomposition of $Tp'(CO)(P(OPh)_3)MoC(O)Et$ (**4b**) occurred when it was heated in THF at 50 °C for 45 min. This thermal degradation could involve phosphite dissociation, so phosphite might be labile at room temperature. Reversible loss of $P(OPh)_3$ was investigated by monitoring a solution of $Tp'(CO)[P(OPh)_3]MoC(O)Et$ (**4b**) and $P(OEt)_3$ by ^{31}P NMR. We reasoned that the smaller alkyl phosphite could compete effectively in trapping any intermediate which would result from loss of $P(OPh)_3$, so the rate of generation of $Tp'(CO)[P(OEt)_3]MoC(O)Et$ (**6**) would reflect the degree of lability of the phosphite ligand. The reverse process, involving treatment of **6** with $P(OPh)_3$, was also examined. Results of these experiments, summarized in Table I, show that phosphite exchange does not occur to an appreciable extent on the time scale of alkylation reactions. This does not directly address questions concerning racemization.

Anionic Enolate Intermediates. Treatment of a red-orange THF solution of the η^2-acyl complex with either excess KH or stoichiometric *n*-BuLi results in a gold solution of the enolate (Scheme III). Formation of the potassium enolate salt was achieved in

Scheme III

$$Tp'(CO)(L)MoC(O)CH_2R \xrightarrow[THF]{KH\ or\ n\text{-}BuLi} M[Tp'(CO)(L)MoC(O){=}CHR] \quad (5)$$

7: R = H, L = CO, M = K^+
8: R = Me, L = $P(OPh)_3$, M = K^+

L = CO, $P(OPh)_3$, $P(OMe)_3$, or $P(OEt)_3$; M = K^+ or Li^+

1 h with excess KH. Deprotonation is essentially instantaneous with *n*-BuLi at −78 °C. Slow addition of *n*-BuLi/hexanes from a syringe was terminated when the red-orange color of the starting acyl complex disappeared. The potassium enolates **7** and **8** have been characterized by IR, ^1H, ^{13}C and ^{31}P NMR spectroscopy. The IR ν(CO) frequencies decrease ca. 100 cm^{-1} upon deprotonation. In **7** the enolate CH_2 protons resonate at δ 3.91 and 4.21 and show no geminal coupling. The carbon of the enolate CH_2 group, C_α, has $^1J_{CH}$ values of 150 and 166 Hz, consistent with resonance forms I and II for enolate **7** in solution.

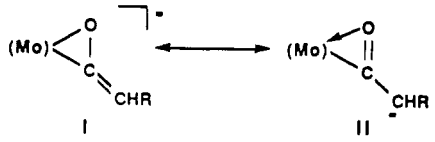

Related anionic η^2-enolate species have been generated by deprotonation of zirconium η^2-acyl precursors.[17] An X-ray structure of $[(\pi\text{-}C_5H_5)_2Zr(CH_3)(\eta^2\text{-}C(O){=}CH_2)]^-$ reflects a

(16) McCleverty, J. A.; Seddon, D.; Bailey, N. A.; Walker, N. W. *J. Chem. Soc., Dalton Trans.* **1976**, 898.

(17) Straus, D. A.; Grubbs, R. H. *J. Am. Chem. Soc.* **1982**, *104*, 5499.

dominant contribution from resonance form I.[18] The ^{13}C chemical shifts of the enolate fragment in both **7** and **8** are similar to those of the η^2-enolate zirconium derivatives.[18] The deprotonated η^2-acyl constitutes an η^2-(C,O)-ketene ligand, and both enolate and ketene nomenclatures appear in the literature.

The ethyl η^2-acyl precursor **4b** has the potential to form both *E* and *Z* isomers upon deprotonation. Only a single isomer of

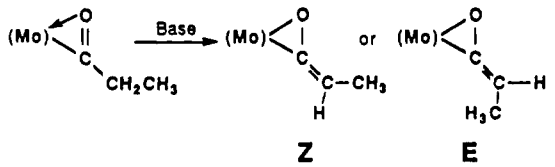

8 is detected by ^1H, ^{13}C, and ^{31}P NMR. Once formed, the enolate appears to be geometrically stable; a sample of **8** in a sealed tube was unchanged after 3 weeks at room temperature. NMR data do not define the configuration of **8** as *Z* or *E* (methyl relative to oxygen). Deprotonation of the related η^2-acyl complex $(\pi\text{-}C_5H_5)_2Zr(CH_3)(C(O)CH_2CH_3)$ results in formation of the less hindered *Z* enolate;[17] the same result may hold for molybdenum enolates.

The rotational preference of the enolate was probed with extended Hückel molecular orbital (EHMO) calculations with simplified octahedral model compounds ($(HCN)_3(CO)(L)MoC(O)=CH_2$ [L = CO, PH_3]). In terms of the ω angle defined by Curtis and illustrated below the minimum energy orientation for

(N_5, *trans* to the acyl, has been omitted for clarity.)

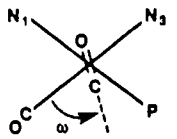

the η^2-enolate ligand was located at $\omega = 45°$ in the dicarbonyl derivative, with a substantial energy difference of 17 kcal/mol relative to the highest energy rotamer. Similar EHMO results for the η^2-formyl model compound $(HCN)_3(CO)_2MoC(O)H$[12] suggest comparable electronic factors for these two ligands. Curtis has lucidly explained the role of octahedral distortions in determining rotational preferences for the η^2-acyl ligand in Tp(CO)-LMo[η^2-C(O)R] complexes.[12]

The rotational energy profile changes only slightly when of one of the carbonyl ligands is replaced with PH_3: the global minimum shifts to $\omega = 55°$. These calculations are in reasonable agreement with the crystallographically determined structure of an acyl product, **12** ($\omega = 71°$), which is described below. In simple terms the acyl carbon is π-acidic, and it prefers to be "cis" to the carbonyls with the hard acyl oxygen closer to a "trans" position relative to the carbonyl ligands.

Alkylation Products. Alkylation at C_α occurs when the enolate reagents are treated with alkyl halides (Scheme IV). Preparation

Scheme IV

$$\underset{\mathbf{2a}}{Tp'(CO)_2MoC(O)Me} \xrightarrow[\text{THF}]{\text{(1) KH, (2) MeI}} \underset{\mathbf{9}}{Tp'(CO)_2MoC(O)C(Me)_3} \quad (6)$$

$$\underset{\mathbf{2b}}{Tp'(CO)_2MoC(O)CH_2CH_3} \xrightarrow[\text{THF}]{\text{(1) n-BuLi (1 equiv), (2) RX (excess)}} Tp'(CO)_2MoC(O)CH(CH_3)R \quad (7)$$

10: R = $PhCH_2$
11: R = $(Me)_3Si$

of the *tert*-butyl η^2-acyl complex **9** demonstrates facile peralkylation in the presence of KH as base and excess alkylating agent (eq 6). The enolate of ethyl acyl **2b** reacted cleanly with benzyl bromide to form $Tp'(CO)_2Mo[C(O)CH(CH_3)(CH_2Ph)]$. The α-silylated acyl complex **11** was prepared by treating the methyl-substituted enolate with Me_3SiCl (eq 7). No products resulting from silicon attack at oxygen were observed.

The elaborated dicarbonyl acyl products are spectroscopically similar to their acyl precursors **2a** and **2b**. NMR spectra reflect equivalence of two pyrazole rings in achiral materials, but if the acyl substituent is chiral then all three pyrazole rings are unique in NMR spectra.

Having elaborated achiral dicarbonyl η^2-acyl complexes, we turned to phosphite-substituted η^2-acyl reagents. Photolysis of $Tp'(CO)_2Mo[C(O)CHMeBz]$ in acetonitrile and addition of $P(OPh)_3$ to the residual material in CH_2Cl_2 produced the substituted product. Chromatography yielded an 80:20 mixture of the two possible diastereomers due to chirality both at carbon and at metal. NMR properties of both diastereomers **12** and **12'** were determined with this mixed sample.

Stereoselective elaboration of the acyl ligand was explored with a racemic mixture of the chiral-at-metal enolate reagent Li-$[Tp'(CO)(P(OPh)_3)MoC(O)=CHCH_3]$ (**8**). Treatment of this enolate with benzyl bromide (BzBr) followed by chromatography produced a single diastereomer (**12**) (eq 8) as monitored by ^1H,

$$\underset{\mathbf{8}}{Li[Tp'(OC)[P(OPh)_3]Mo(C(O)=CHMe)]} + BzBr \rightarrow \underset{\mathbf{12}}{Tp'(OC)[P(OPh)_3]MoC(O)CHMeBz} + LiBr \quad (8)$$

^{13}C, and ^{31}P NMR. The selectivity of the alkylation was assayed more directly by recording a ^{31}P NMR spectrum of the reaction solution after the lithium enolate reagent was transferred into excess benzyl bromide at 0 °C. Only one signal was detected in the ^{31}P NMR spectrum of the crude material. The $P(OPh)_3$ derivative was more selective than either the $P(OEt)_3$- or the $P(OMe)_3$-substituted enolates as indicated by the diastereomer ratios for benzylation reactions with L = $P(OPh)_3$, $P(OEt)_3$, and $P(OMe)_3$ presented in Table II.

Confirmation that the alkylation reaction is kinetically controlled was obtained by treating deprotonated $Tp'(CO)(P(OPh)_3)MoC(O)CH_2CH_2Ph$ with MeI. Only the opposite diastereomer, **12'**, was detected by ^1H NMR after chromatography.

A crystalline sample of **12** was obtained by reacting the enolate with excess BzBr in THF. Concentration of the solution produced single crystals. The relative configuration of the chiral metal and carbon centers was determined by X-ray diffraction analysis; the molecular structure of $Tp'(CO)[P(OPh)_3]Mo(\eta^2\text{-}C(O)CHMeBz)$, **12**, is depicted in Figure 1. The molybdenum coordination sphere is seen more clearly on the right where the phenyl and pyrazole rings have been omitted. Selected bond distances are listed in Table III.

The structure of $Tp'(CO)[P(OPh)_3]Mo(\eta^2\text{-}C(O)CHMeBz)$ is roughly octahedral if one relegates the η^2-acyl ligand to a single

Table II. Enolate Alkylation Selectivity Ratios

$Li[Tp'(CO)LMoC(O)R] + R'X \rightarrow Tp'(CO)LMoC(O)CH(CH_3)CH_2Ph$

L	R	R'X	selectivity
$P(OPh)_3$	$CHCH_3$	$PhCH_2Br$	>98:2
$P(OPh)_3$	$CHCH_2Ph$	CH_3I	>2:98
$P(OEt)_3$	$CHCH_3$	$PhCH_2Cl$	96:4
$P(OMe)_3$	$CHCH_3$	$PhCH_2Br$	80:20

Table III. Selected Bond Distances for $Tp'(CO)(P(OPh)_3)MoC(O)CH(CH_3)CH_2Ph$ (**12**)

atoms	distance, Å	atoms	distance, Å
Mo–P	2.399 (2)	Mo–C(1)	1.86 (1)
Mo–C(2)	1.996 (9)	O(1)–C(1)	1.24 (1)
Mo–O(2)	2.201 (5)	O(2)–C(2)	1.257 (8)
Mo–N(1)	2.200 (7)	P–O(3)	1.602 (5)
Mo–N(3)	2.277 (6)	P–O(4)	1.611 (5)
Mo–N(5)	2.231 (6)	P–O(5)	1.647 (5)

(18) (a) Ho, S. C. H.; Straus, D. A.; Armantrout, J.; Schaefer, W. P.; Grubbs, R. H. *J. Am. Chem. Soc.* **1984**, *106*, 2210. (b) Moore, E. J.; Straus, D. A.; Armantrout, J.; Santarsiero, B. D.; Grubbs, R. H.; Bercaw, J. E. *J. Am. Chem. Soc.* **1983**, *105*, 2068.

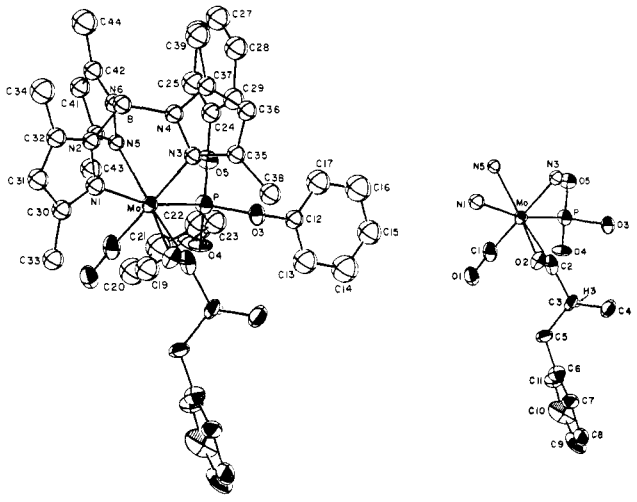

Figure 1. An ORTEP plot of $Tp'(CO)[P(OPh)_3]Mo[\eta^2-C(O)CHMeBz]$ (**12**) with an inset showing the coordination sphere and η^2-acyl ligand.

coordination site. Seminal work by Lalor and Ferguson provides two comparable η^2-acyl structures of $Tp'(CO)_2Mo[\eta^2-C(O)R]$.[19] Curtis and co-workers provided a thorough analysis of η^2-acyl structures in 1986.[12] Metrical data for the η^2-acyl product here is similar to six molybdenum η^2-acyl complexes included in Curtis' summary table. The Mo–C distance of 2.00 Å and Mo–O distance of 2.20 Å differ by 0.20 Å; this value of $\Delta[d(M-O) - d(M-C)]$ is typical of group six η^2-acyl complexes. Larger Δ values are common for later transition metals, while early metals tend to be more oxophilic and display smaller or even negative Δ values. A recent exception is an iron η^2-acyl product resulting from CO insertion into $(dippe)FeR_2$ with $\Delta = 0.10$ Å.[20]

The Mo–N distances reflect the trans influence of CO, the η^2-acyl ligand, and $P(OPh)_3$ at 2.28, 2.23, and 2.20 Å, respectively. Average Mo–N bond lengths are 2.24, 2.19, and 2.22 Å for four $Tp(CO)LMo[\eta^2-C(O)Me]$ complexes for the nitrogen donor trans to CO, C(O)Me, and L (L = $P(OMe)_3$ and PEt_3), respectively.[12]

The orientation of the η^2-acyl group is important in stereoselective reactions. Here $\omega = 71.3°$; this qualitatively aligns the acyl CO axis near the phosphite–metal–pyrazole axis, P–Mo–N1. The acyl carbon is near the phosphite, and the oxygen is near N1. Values of $\omega = 69$ and -77 for PEt_3 and $P(OMe)_3$ Tp analogues[12] indicate that alignment near the P–Mo–N bond is observed in each case, but the O–C orientation is variable.

In **12** the 164.2° P–Mo–N1 angle compares to the 175.2° Cl–Mo–N3 angle to confirm the deformation pattern rationalized by Curtis.[12] As predicted the acyl lines up over the distorted P–Mo–N axis to optimize π-interactions.

The flexibility of the Tp′ ligand is reflected in the deviation of the three pyrazole rings from C_3 symmetry. Angles between adjacent pyrazole planes are 104.6°, 120.3°, and 134.9° to accommodate the carbonyl, η^2-acyl, and triphenyl phosphite ligands, respectively. Larger groups occupy larger gaps. In the $Tp(CO)LMo(\eta^2-C(O)Me)$ derivatives angles of 132 and 138° between pyrazole planes accommodate $P(OMe)_3$ and PEt_3 ligands, respectively.[12]

The structure of this product suggests a simple model for predicting π-facial selection in molybdenum η^2-enolates. This system can be related to models for nucleophilic attack on carbonyl compounds[21] and to reactions of iron η^1-enolates with electrophiles.[4]

It seems likely that the electrophile will approach the least hindered enolate face preferentially, i.e., from the carbonyl ligand side. Scheme V illustrates two possibilities which would result in the relative stereochemistry observed for **12**. Case A assumes

Scheme V

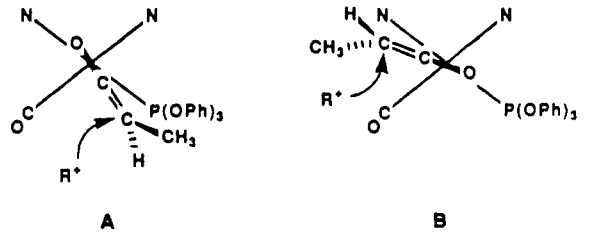

(N *trans* to the acyl ligand is omitted for clarity.)

Scheme VI

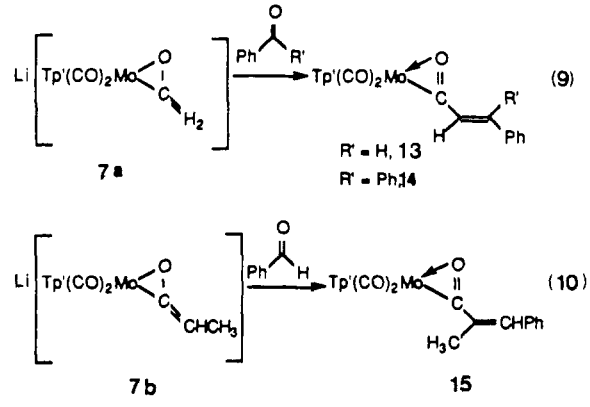

that the rotational preference of the enolate is the same as that of the acyl ligand in **12**, with the enolate CO vector roughly parallel to the Mo–P vector and carbon adjacent to the phosphite. Approach of RX from the least hindered side of the (*Z*)-enolate would lead directly to the observed product. Since the geometry of the enolate is not explicitly known, reactivity involving the (*E*)-enolate must also be considered. In this case, approach of the electrophile over the carbonyl ligand would require the enolate moiety to be rotated 180° from the preferred acyl orientation in order to produce the relative stereochemistry observed in **12**. Regardless, the $P(OPh)_3$ ligand presumably blocks approach of the electrophile to one of the enolate faces and directs the stereoselective alkylation of the enolate moiety.

Aldol Condensation Products. Dicarbonylmolybdenum η^2-enolates **7** and **8** react with PhCHO to give α,β-unsaturated η^2-enone products (Scheme VI), and enolate **7a** condenses with Ph_2CO to form the η^2-diphenylenone species **14**.

Photolytic replacement of one CO ligand in **15** with $P(OPh)_3$ results in two isomeric phosphite substituted η^2-enone complexes (**16** and **16′**, probably geometric *Z,E* isomers about the vinyl double bond) and a trace of the dicarbonyl π-allyl species **17** (eq 11).

$$Tp'(CO)_2MoC(O)C(CH_3){=}CHPh \xrightarrow[\text{(2) L = P(OPh)}_3]{\text{(1) h}\nu\text{, CH}_3\text{CN}} \underset{\mathbf{16},\ \mathbf{16'}\ (75:25)}{Tp'(CO)(L)MoC(O)C(CH)_3{=}CHPh} + \underset{\mathbf{17}\ (\text{trace})}{Tp'(CO)_2Mo(\eta^3\text{-}CH_2CHCHPh)} \quad (11)$$

The α,β-unsaturated enone products have ν CO stretches near 1940 and 1830 cm^{-1} and a weak ν_{CC} stretch near 1600 cm^{-1}. The two pyrazole rings opposite the CO ligands are NMR equivalent. Protons attached to C_α and C_β resonate in the 7.5–8.0 ppm region, and the vicinal coupling constant for these olefinic protons ($^3J_{HH}$ = 15.7 Hz) establishes an *E* or trans geometry in **13**. In **15** the coupling of $^4J_{HH}$ = 1.2 Hz is consistent with either an *E* or *Z* configuration. NMR data for compounds **13** and **15** indicate that only one geometric isomer is formed in each case. In all three α,β-unsaturated compounds the η^2-carbonyl was identified by long-range proton coupling; the two carbon monoxide carbons resonate in the 230–240 ppm region. The vinyl C_α is 19–36 ppm

(19) Desmond, T.; Lalor, F. J.; Ferguson, G.; Ruhl, B.; Parvez, M. *J. Chem. Soc., Chem. Commun.* **1983**, 55.
(20) Hermes, A. R.; Girolami, G. S. *Organometallics* **1988**, *7*, 394.
(21) Eliel, E. in *Asymmetric Synthesis*, J. D. Morrison, Ed.; Academic Press, New York, 1983; Vol. 2, p 125.

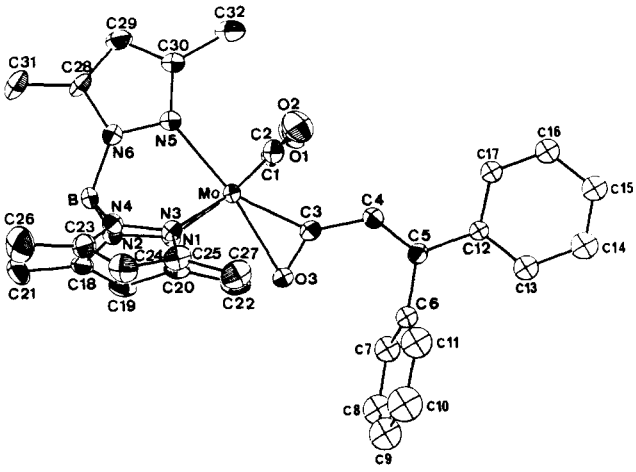

Figure 2. An ORTEP plot of $Tp'(CO)_2Mo[\eta^2\text{-}C(O)CH{=}CPh_2]$ (**14**).

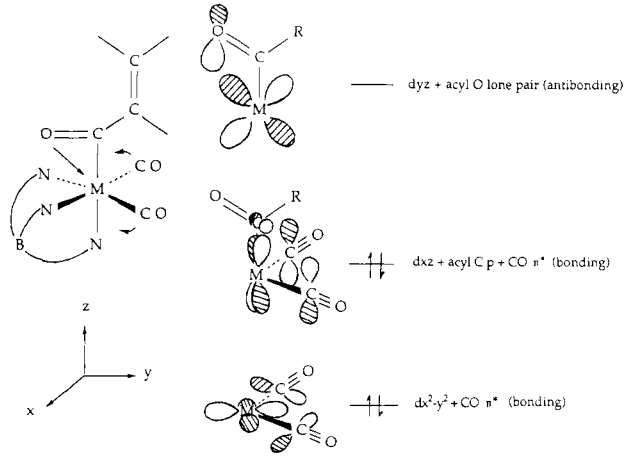

Figure 3. Metal $d\pi$-ligand orbital interactions in $Tp'(CO)_2Mo[\eta^2\text{-}C(O)CH{=}CPh_2]$ with the OC–Mo–CO angle greater than 90° dictating that d_{xz} will lie below d_{yz} in energy.

Table IV. Selected Bond Distances for $Tp'(CO)_2MoC(O)CH{=}CPh_2$ (**14**)

atoms	distance, Å	atoms	distance, Å
Mo–C(1)	1.948 (5)	C(1)–O(1)	1.162 (7)
Mo–C(2)	1.940 (6)	C(2)–O(2)	1.166 (5)
Mo–C(3)	1.982 (4)	C(3)–O(3)	1.235 (4)
Mo–O(3)	2.275 (3)	C(3)–C(4)	1.453 (5)
Mo–N(1)	2.219 (3)	C(4)–C(5)	1.338 (5)
Mo–N(3)	2.202 (4)	C(5)–C(6)	1.500 (5)
Mo–N(5)	2.182 (4)	C(5)–C(12)	1.492 (5)

upfield from C_β, a common feature in α,β-unsaturated ketones.[22]

An ORTEP diagram of the structure of the η^2-diphenylenone **14** is presented in Figure 2, and bond distances are listed in Table IV. The geometry of $Tp'(CO)_2Mo(\eta^2\text{-}C(O)CH{=}CPh_2)$ conforms to established patterns for six-coordinate d^4 cis dicarbonyl complexes. The OC–Mo–CO angle determines which two $d\pi$ orbitals will be stabilized and hold the four metal electrons.[23,24] The obtuse 96° OC–M–CO angle here suggests that the only vacant $d\pi$ orbital will be the vertical one between the cis CO's, and it can serve as an acceptor orbital for donation from an oxygen lone pair (Figure 3). Indeed the acyl ligand lies nearly midway between the two CO ligands on the approximate symmetry plane. This positions the acyl carbon perpendicular p orbital to overlap with the filled

(22) Silverstein, R. M.; Bassler, G. C.; Morrill, T. C. *Spectrometric Identification of Organic Compounds*, 4th ed.; J. Wiley, New York, 1981; p 263.

(23) Kubacek, P.; Hoffmann, R. *J. Am. Chem. Soc.* **1981**, *103*, 4320.

(24) (a) Templeton, J. L.; Winston, P. B.; Ward, B. C. *J. Am. Chem. Soc.* **1981**, *103*, 7713. (b) Templeton, J. L.; Ward, B. C. *J. Am. Chem. Soc.* **1980**, *102*, 6568.

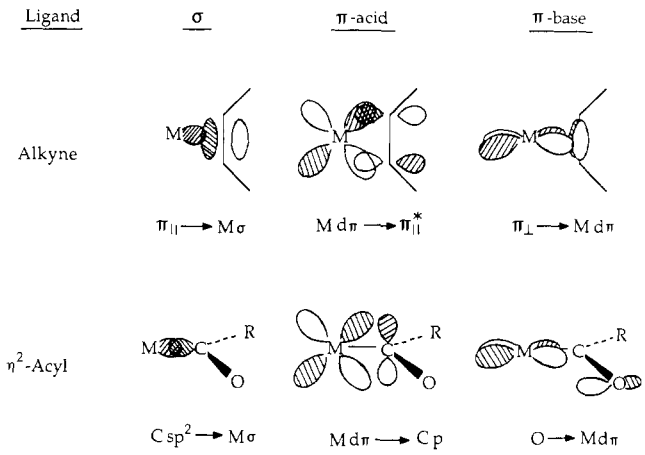

Figure 4. Pictorial representation of the crude orbital analogy between four-electron alkyne ligands and η^2-acyl ligands. The MC(O)R plane is orthogonal to the M(RC≡CR) plane.

Scheme VII

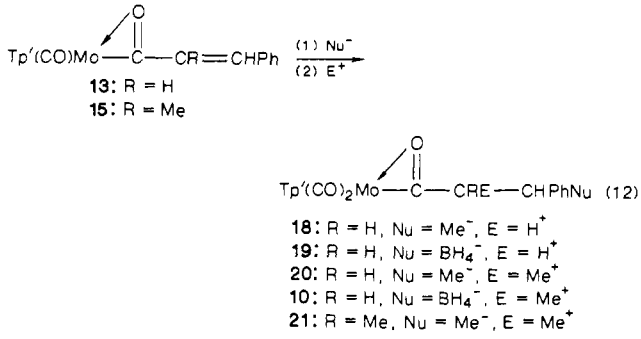

orthogonal $d\pi$ level. The single-faced π-donor and π-acceptor properties of η^2-acyl ligands mimic four-electron alkyne ligands;[25] the preferred orientation of the C≡C and C=O fragments will be orthogonal to one another. Simply stated alkynes and η^2-acyls both have σ-donor ($\pi_\parallel$ and C sp^2), π-acceptor (π^* and C_p), and π-donor ($\pi_\perp$ and 0 lone pair) functions (Figure 4).

Bond distances in the metal–η^2-acyl unit are important in assessing delocalization. The Δ of 0.29 Å [d(M–O) − d(M–C)] in **14** is 0.09 Å larger than in acyl **12** and is close to the high end of the Δ range reported to date.[12] The enone backbone distances run 1.24 Å (O=C), 1.45 Å (C–C), and 1.34 Å (C=C) with 1.50 and 1.49 Å distances to the pendant phenyl groups; the enone has only a small contribution from resonance form II.

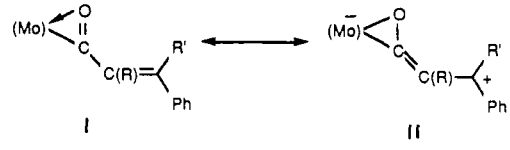

Conjugate Addition Products. The dicarbonyl η^2-enone complex **13** undergoes nucleophilic attack at C_β which can be followed by electrophilic addition at C_α to yield saturated η^2-acyls (Scheme VII). Methyl lithium or sodium borohydride was used as nucleophile, and water or methyl iodide was used as quencher. No products resulting from nucleophilic attack at the η^2-carbonyl carbon were detected.

When $K[HB(OPr^i)_3]$ reacts with $Tp'(OC)_2Mo[\eta^2C(O)CH{=}CHPh]$ a gold intermediate is generated with ν_{CO} stretches at 1912 and 1723 cm^{-1}, quite similar to the IR pattern of $K[Tp'(OC)_2Mo(\eta^2\text{-}C(O){=}CH_2)]$. This gold intermediate reacts rapidly with MeI to form $Tp'(OC)_2Mo(\eta^2\text{-}C(O)CHMeCH_2Ph)$.

Thermal Formation of an Allyl Complex from an η^2-Enone Complex. The η^2-enone complex **15** slowly loses CO in refluxing

(25) Brower, D. C.; Birdwhistell, K. R.; Templeton, J. L. *Organometallics* **1986**, *5*, 94.

Scheme VIII

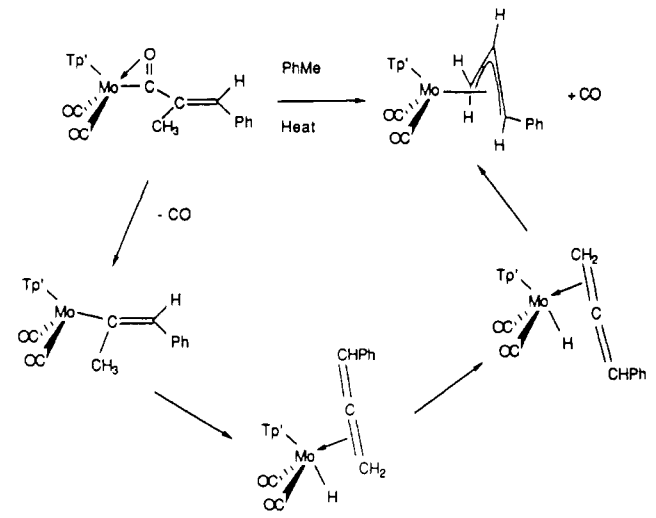

Scheme IX

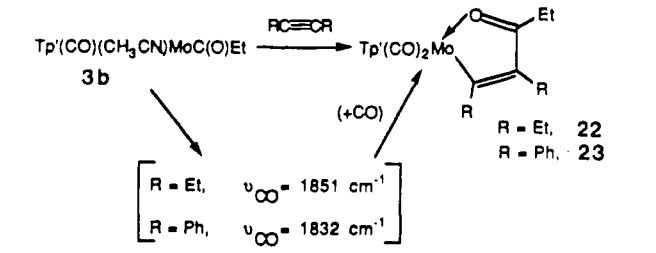

toluene to form an η^3-allyl product, $Tp'(CO)_2Mo(\eta^3-CH_2CHCHPh)$, **17** (eq 13). Compound **17** has equal intensity

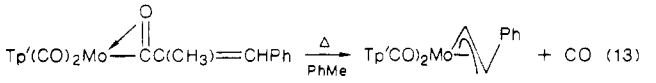

17

ν_{CO} bands at slightly lower energy than the η^2-enone starting material. The ^1H and ^{13}C NMR spectra of **17** indicate an η^3-allyl formulation, and all three allyl carbons exhibit $^1J_{CH}$ values of 160–166 Hz. The position of the phenyl group was determined by comparison of proton couplings in **17** with those of monosubstituted η^3-allyl ligands in the $(\pi\text{-Cp})Mo(CO)_2$ system[26] (see Table V). Couplings between the anti protons and the central proton ($^3J_{HaHc}$ and $^3J_{Ha'Hc}$) tend to be ca. 8–10 Hz, while the syn couplings ($^3J_{HsHc}$ and $^3J_{Hs'Hc}$) are usually 6–8 Hz. Two J_{HH} couplings near 10 Hz here suggests that protons occupy both anti positions in the π-allyl ligand. The absence of syn coupling in **17** (usually $^4J_{HsHs'}$ = 1–2 Hz) also indicates that the phenyl group occupies a syn position.

Rearrangement of the α-methyl η^2-enone complex to an η^3-allyl product is reminiscent of Green's rearrangement of methyl substituted vinyl species to η^3-allyl products.[27] Nucleophilic attack on $[Cp[P(OMe)_3]_2Mo(MeC{\equiv}CMe)]^+$ at an alkyne carbon generates an 18-electron η^2-vinyl complex.[28] Labeling studies are compatible with hydrogen transfer from the vinyl methyl group to the adjacent carbon to form an allyl ligand. Attractive intermediates are accessible by η^2-vinyl to η^1-vinyl conversion then β-hydrogen migration to form a metal allene hydride and finally allyl formation by hydrogen transfer to the central allene carbon.

Thermal loss of a terminal carbonyl ligand from $Tp'(OC)_2Mo(\eta^2-C(O)CMe{=}CHPh)$ followed by migration of the

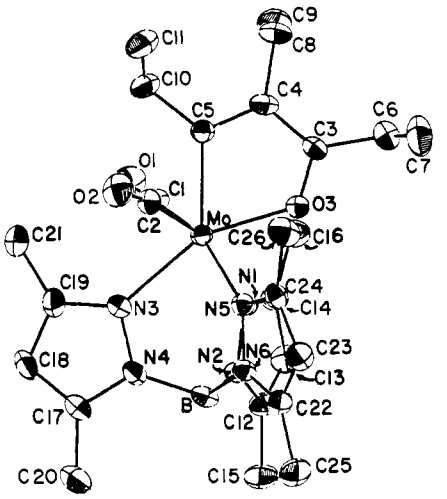

Figure 5. An ORTEP plot of $Tp'(CO)_2Mo(CEtCEtC(O)Et)$ (**22**).

Scheme X

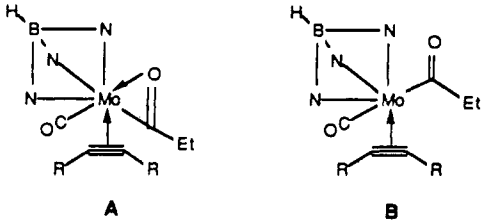

enone vinyl group to the metal could form an analogue of Green's vinyl complex. β-Hydride transfer to molybdenum from the vinyl methyl substituent and subsequent migration of the metal hydride to the central carbon of the π-allene ligand would be analogous to Green's proposed mechanism (Scheme VIII).

Alkyne Insertion Products. The η^2-acyl complex $Tp'(CO)(CH_3CN)MoC(O)Et$ (**3b**) reacts with alkynes to form a monocarbonyl intermediate which decomposes to dicarbonyl metallacyclic products (**22** or **23**) in 20–40% yield (Scheme IX). The yield of the alkyne insertion product is increased by addition of carbon monoxide after formation of the monocarbonyl intermediate.

The two CO ligands in **22** and **23** produce IR bands separated by about 90 cm^{-1}. The CO ligands are homotopic in ^{13}C NMR spectra of both **22** and **23**, and the pyrazole rings opposite the carbonyls are also NMR equivalent. In the oxametallacycle the olefinic C_β resonates at δ 135, the ketonic carbon C_γ at δ 192, and C_α is seen near δ 250. Similar values characterize alkyne insertion products in Alt's $(\pi\text{-}C_5H_5)(CO)_3MR$ system.[29] The carbene-like character of C_α is evident in the low field chemical shift.[30]

IR evidence suggests that the alkyne initially replaces CH_3CN to give a monocarbonyl intermediate which then rearranges to the final product. The intermediate is probably either an η^2-acyl complex with a two-electron donor alkyne (A) or an η^1-acyl four-electron donor alkyne complex (B). NMR data for the related complex $(\pi\text{-}C_5H_5)(CO)(HCCH)WC(O)Et$ favor the η^1-acyl/four-electron donor alkyne formulation.[31]

Substantial work with alkyne insertion into the metal–acyl bond of $CpM(CO)_2C(O)R$ has been reported.[29,32] More recently similar products have been observed with alkyne addition following CO insertion into the tungsten–alkyl bond of an enolate derivative, $Cp(CO)_3WCH_2CO_2Et$.[33]

(26) (a) Pannell, K. H.; Lappert, M. F.; Stanley, K. *J. Organomet. Chem.* **1976**, *112*, 37. (b) Merour, J. Y.; Charrier, C.; Benaim, J.; Roustan, J. L.; Commereuc, D. *J. Organomet. Chem.* **1972**, *39*, 321.
(27) Green, M. *J. Organomet. Chem.* **1986**, *300*, 93.
(28) Allen, S. R.; Baker, P. K.; Barnes, S. G.; Bottrill, M.; Green, M.; Orpen, A. G.; Williams, I. D.; Welch, A. J. *J. Chem. Soc., Dalton Trans.* **1983**, 927.
(29) Alt, H. G.; Engelhardt, H. E.; Thewalt, U.; Riede, J. *J. Organomet. Chem.* **1985**, *288*, 165.
(30) Allen, S. R.; Green, M.; Norman, N. C.; Paddick, K. E.; Orpen, A. G. *J. Chem. Soc., Dalton Trans.* **1983**, 1625.
(31) (a) Alt, H. G.; Eichner, M. E.; Jansen, B. M. *Angew. Chem. Suppl.* **1982**, 1826. (b) Alt, H. G. *J. Organomet. Chem.* **1977**, *127*, 349.
(32) (a) Davidson, J. L.; Green, M.; Nyathi, J. Z.; Scott, C.; Stone, F. G. A.; Welch, A. J.; Woodward, P. *J. Chem. Soc., Chem. Commun.* **1976**, 714. (b) Watson, P. L.; Bergman, R. G. *J. Am. Chem. Soc.* **1979**, *101*, 2055.

Table V. ^{1}H NMR Data for n^3-Allyl Complexes of Mo(II)

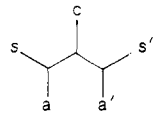

complex, (Mo′) = (π-C_5H_5)Mo(CO)$_2$	H_a	$H_{a'}$	H_s	$H_{s'}$	H_c	ref
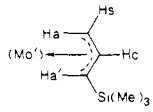	0.94 J_{ac} = 10.0 J_{as} = 1.4 $J_{aa'}$ = 0.3	0.37 $J_{a'c}$ = 12.4 $J_{a'a}$ = 0.3	2.58 J_{sc} = 6.0 J_{sa} = 1.4		3.60 (m)	26a
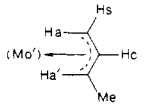	1.26 J_{ac} = 10.2 J_{as} = 2.2	1.75 $J_{a'c}$ = 7.9 $J_{a's}$ = 0.3	2.54 J_{sc} = 6.8 J_{sa} = 2.2		3.90 (m)	26b
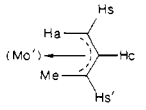	1.32 J_{ac} = 10.2 J_{as} = 2.6		2.80 J_{sc} = 7.0 J_{sa} = 2.6 $J_{ss'}$ = 1.9	3.83 $J_{s'c}$ = 7.9 $J_{s'c}$ = 1.9	4.0 (m)	26b
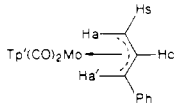	2.06 J_{ac} = 10.3 J_{as} = 1.0	4.22 $J_{a'c}$ = 9.8	3.67 J_{sc} = 6.8 J_{sa} = 1.0		5.37 (m)	this work

Table VI. Selected Bond Distances for Tp′(CO)$_2$Mo$\overline{\text{C(Et)C(Et)C(O)}}$Et (**22**)

atoms	distance, Å	atoms	distance, Å
Mo–O(3)	2.051 (2)	O(3)–C(3)	1.287 (4)
Mo–C(5)	2.166 (3)	C(3)–C(4)	1.361 (5)
Mo–N(1)	2.252 (3)	C(3)–C(6)	1.491 (5)
Mo–N(3)	2.230 (3)	C(4)–C(5)	1.366 (5)
Mo–N(5)	2.247 (3)	C(4)–C(8)	1.534 (5)
Mo–C(1)	1.942 (4)	C(5)–C(10)	1.509 (5)
Mo–C(2)	1.952 (4)	C(6)–C(7)	1.464 (7)
O(1)–C(1)	1.156 (4)	C(8)–C(9)	1.526 (6)
O(2)–C(2)	1.151 (4)	C(10)–C(11)	1.550 (5)

The crystal structure of Tp′(CO)$_2$Mo$\overline{\text{[CEtCEtC(O)}}$Et] revealed that the oxametallacycle adopts an orientation perpendicular to that found in related cyclopentadienyl complexes (Figure 5). Bond distances for **22** are listed in Table VI. Compound **22** approaches a face-capped octahedral geometry, with the three bound nitrogens (N1, N3, and N5), the terminal carbonyls (C1 and C2), and the ketonic oxygen (O3) defining the vertices of the octahedron and C5, the α-carbon of the metallacycle, forming the cap. The dihedral angles between the planes of the dmpz rings are all near 120°. The angles between the metal-bound nitrogens are slightly less than 90°, while the angles between the carbonyls and the ketonic oxygen are 100–115°.

The planar metallacycle lies on a pseudo-symmetry plane which contains the N$_3$ dmpz ring and bisects ∠O(1)C(1)–Mo–C(2)O(2). I and II are canonical forms which represent bonding within the metallacycle. The C(3)–O(3) distance (1.29 Å) falls between typical C–O single bond and C=O double bond distances. Bond distances C(3)–C(4) and C(4)–C(5) are nearly equal, reflecting resonance contributions from both I and II. Multiple Mo–C(5) bond character due to resonance form II is apparent in both the Mo–C(5) bond (2.17 Å)[34] and in the low-field chemical shift of C(5).

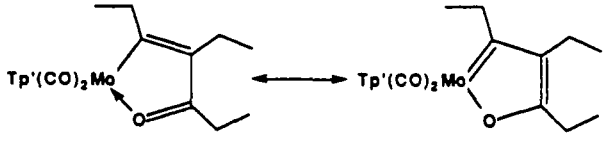

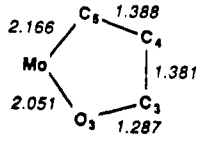

A structural comparison of **22** with a π-Cp complex containing a similar metallacyclic ligand[29] reveals one significant difference: the π-Cp complex adopts a "four-legged piano stool" geometry with the metallacyclic ligand rotated approximately 90° from the position observed for **22**. Equivalence of the terminal CO ligands in NMR spectra of π-Cp metallacyclic complexes indicates that these species have effective C_s symmetry in solution, so the energy barrier for rotation of the chelating organic ligand is small. Bonding electrons in the tripodal Tp′ ligand are more localized than those associated with π-C_5H_5;[12] this feature may be important in the structural differences between **22** and related π-Cp complexes.

Summary and Conclusions

Clean enolate formation with simple bases such as BuLi or KH from Tp′(CO)$_2$Mo[C(O)CH$_3$] reagents contrasts with results reported for the parent Tp(CO)$_2$Mo[C(O)CH$_3$] complex. Substantial chemical differences between Tp and Tp′ complexes have been observed previously.[20,35] In the three structures reported here, the Mo atom lies near the plane of the three pendant 3-methyl groups of the Tp′ ligand. Certainly access to the metal center is restricted substantially by the pyrazolyl methyl substituents.

Excellent diastereoselectivity has been demonstrated for enolate alkylation with racemic metal reagents. One attractive feature of η^2-acyl reagents is that the internal Lewis acid role of molybdenum eliminates counter ion effects which are otherwise important variables in enolate reactions. Why have we chosen not to invest effort in resolution of enantiomers nor in freeing the organic fragment from the metal, two crucial requisites for synthetic applications? Our interest has been in identifying fundamental ligand transformation reactions. We don't foresee major advantages for the Tp′L(CO)Mo(η^2-C(O)R) system relative to

(33) Burkhardt, E. R.; Doney, J. J.; Bergman, R. G.; Heathcock, C. H. *J. Am. Chem. Soc.* **1987**, *109*, 2022.

(34) Bennett, M. J.; Mason, R. *Proc. Chem. Soc.* **1963**, 273.

(35) (a) Bruce, A. E.; Gamble, A. S.; Tonker, T. L.; Templeton, J. L. *Organometallics* **1987**, *6*, 1350. (b) Ghosh, C. K.; Graham, W. A. G. *J. Am. Chem. Soc.* **1987**, *109*, 4726.

organic alternatives for diastereoselective enolate alkylation reactions.

Addition of benzaldehyde to enolate reagents and elimination forms η^2-enone complexes. Conjugate addition reactions to the η^2-enone complexes work well. Another η^2-enone ligand based reaction is decarbonylation with concomitant rearrangement, by net hydrogen transfer from an α-methyl substituent, to form an η^3-allyl complex. These η^2-enone reactions pose additional questions. Are conjugate addition reactions stereoselective when the metal is chiral? What products form when η^2-enone complexes without hydrogen-bearing groups in the α position are decarbonylated? Alkyne insertion into a metal–acyl carbon bond to form a five-membered metallacycle has also been observed. Carbene character is evident in structural data for the $Tp'(CO)_2Mo{=}(CEtCEtC(O)Et)$ complex.

Reactions of η^2-acyl ligands in these d^4 Mo(II) complexes span an impressive range of ligand transformations. This extensive chemistry is made possible by (1) the steric bulk of the Tp′ ligand which inhibits reactions at the metal center and (2) the electronic effects of binding the acyl oxygen to the metal in an intramolecular fashion.

Experimental Section

General Methods. Manipulations involving air-sensitive reagents were performed under nitrogen using Schlenk techniques. Solvents were purified as follows: CH_2Cl_2 was distilled from CaH_2; Et_2O, THF, toluene, and hexanes were distilled from potassium benzophenone ketyl. CH_3CN, Me_2CO, MeI and EtI were purified by swirling over activated alumina for several minutes and then purged with nitrogen. Alkyl phosphites were distilled from potassium. A mineral oil suspension of KH was washed thoroughly with hexanes and then dried under vacuum prior to use. Dimethylpyrazole,[36] KTp′,[37] and $K[Tp'Mo(CO)_3]$ (**1**)[16] were prepared by literature methods. All other reagents were purchased from commercial sources and used without further purification. Infrared spectra were recorded on a Beckman IR-4250 spectrometer and calibrated with a polystyrene standard. NMR spectra were recorded on Bruker WM-250 (250 MHz) or AC-200 (200 MHz) spectrometers. When necessary, homonuclear decoupling experiments were employed to extract coupling constants from ^1H NMR spectra. Resolution enhancement experiments were performed to quantify small couplings. All ^{31}P NMR spectra were obtained in either ^1H broad band or ^1H "waltz-decoupled" mode. Chemical shifts were referenced to residual solvent protons for ^1H NMR, to solvent for ^{13}C NMR, and to external aqueous H_3PO_4 (85%) for ^{31}P NMR spectra. Complete NMR data is available as Supplementary Material. Microanalyses were performed by Galbraith Laboratories, Knoxville, TN.

All photolyses were carried out in a submersion type photolysis reactor at 0 °C using a Hanovia 750 W medium pressure Hg arc lamp. Solutions were stirred and purged with nitrogen during photolysis.

Syntheses. $Tp'(CO)_2MoC(O)R$ [R = Me, 2a; R = Et, 2b]. A slurry of $Mo(CO)_6$ (7.92 g, 30.0 mmol) and potassium hydridotris(3,5-dimethylpyrazolyl)borate (KTp′, 10.09 g, 30.0 mmol) in 150 mL of THF was refluxed for 18 h. MeI (19 mL, 305 mmol) was added, and the mixture was refluxed for 22 h. The deep red solution volume was then reduced to 100 mL, and 200 mL of hexanes was added. After the salt settled, the supernatant was transferred by cannula to a 5 × 8 cm column of alumina. The residual salt was washed with 4 × 50 mL of hexanes and then 5 × 20 mL hexanes/methylene chloride (50%). The orange-red product was eluted with hexanes/30% methylene chloride and stripped to an orange powder (13.1 g, 26.5 mmol, 89%). Both **2a** and **2b** were relatively air stable as solids, but solutions turned brown after a few minutes in air. The ethyl η^2-acyl complex was moderately soluble in alkanes and acetonitrile and very soluble in most other organic solvents. **$Tp'(CO)_2MoC(O)Me$ (2a)** (70% yield after chromatography): IR (KBr) ν_{BH} 2518 vw; ν_{CO} 1962 s, 1833 vs; ν_{CN} 1538 m; ^1H NMR (CD_3CN) δ 2.02, 2.21, 2.24, 2.45 (4s, 6:3:6:3 H, Tp′CH_3), 3.30 (s, 3H, —C(O)CH_3), 5.89, 5.95 (2s, 2:1 H, Tp′ C—*H*); ^{13}C NMR (CD_3CN) δ 12.7, 13.5, 13.6, 15.4 (4q, Tp′ CH_3), 28.5 (q, $^1J_{CH}$ = 131 Hz, —C(O)CH_3), 107.5, 108.2 (2d, $^1J_{CH}$ = 175 Hz, Tp′*C*—H), 146.1, 148.3, 152.5, 153.7 (4 m, Tp′*C*—CH_3), 232.8 (s, *CO*), 252.5 (q, $^2J_{CH}$ = 6 Hz, —*C*(O)CH_3); Calcd C, 46.38; H, 5.08; N, 17.08. Obsd C, 46.49; H, 4.95; N, 17.12. **$Tp'(CO)_2MoC(O)Et$ (2b)** (50% yield after chromatography): IR (KBr) ν_{BH} 2520 vw; ν_{CO} 1961 s, 1828 vs, ν_{CN} 1535 m; ^1H NMR (CD_2Cl_2) δ 1.59 (t, $^3J_{HH}$ = 7 Hz, 3 H, —CH_2CH_3), 3.78 (q, $^3J_{HH}$ = 7 Hz, 2 H, CH_2CH_3); ^{13}C NMR (CD_2Cl_2) 232.2 (s, *CO*), 253.7 (t, $^2J_{CH}$ = 5 Hz —*C*(O)-CH_2—). Calcd: C, 47.47; H, 5.34; N, 16.61. Obsd: C, 47.35; H, 5.35; N, 16.93.

$Tp'(CO)(L)MoC(O)R$ [L = $P(OPh)_3$, R = Me, 4a; L = $P(OPh)_3$, R = Et, 4b; L = $P(OMe)_3$, R = Et, 5; L = $P(OEt)_3$, R = Et, 6]. The following procedure is representative for the phosphite-substituted acyl complexes **4a**, **4b**, **5**, and **6**. A CH_3CN solution of $Tp'(CO)_2MoC(O)Et$ (**2b**, 4.56 g, 9.00 mmol) was photolyzed with a nitrogen purge at 0 °C until the reaction was about 80% complete as judged by IR (about 6 h). The solvent was removed, and the resulting burgundy paste was dissolved in 90 mL of CH_2Cl_2. $P(OMe)_3$ (1.3 mL, 10.8 mmol) was added, and the deep red solution was stirred for 30 min before removing the solvent under vacuum. The resultant red oil was dissolved in benzene and chromatographed on alumina. Excess $P(OMe)_3$ was first washed from the column with hexanes. Hexanes/5% Et_2O as eluent provided two orange fractions. The first fraction yielded 0.45 g (0.89 mmol) of starting material. The second fraction contained 3.40 g of $Tp'(CO)(P(OMe)_3)MoC(O)Et$ (**5**, 5.65 mmol, 70% yield based on starting material consumed). The phosphite-substituted acyl complexes are orange powders. They are insoluble in alkanes but dissolve in most other organic solvents. The complexes, especially the $P(OPh)_3$ derivatives, display moderate thermal sensitivity in solution and decompose when heated at temperatures above 40–50 °C for prolonged periods.

$Tp'(CO)(CH_3CN)MoC(O)R$ [R = Me, 3a; R = Et, 3b]: IR (CH_3CN) ν_{CO} 1774 s.

$Tp'(CO)(P(OPh)_3)MoC(O)Me$ (4a) (50% yield after chromatography): IR (KBr) ν_{BH} 2520 w, ν_{CO} 1797 s, ν_{CC} 1588 m, ν_{CN} 1541 m; ^1H NMR (CD_2Cl_2) δ 1.80, 2.02, 2.08, 2.31, 2.32, 2.44 (6s, each 3 H, Tp′CH_3), 3.53 (s, 3 H, —C(O)CH_3), 5.19, 5.82, 5.88 (3s, each 1 H, Tp′ C—*H*), 6.63–7.33 (m, 15 H, $P(OC_6H_5)_3$); ^{13}C NMR (CD_2Cl_2) δ 12.9, 13.9, 15.5, 15.9 (4q, Tp′CH_3), 28.7 (q, $^1J_{CH}$ = 131 Hz, —C(O)CH_3), 106.5, 107.6, 107.9 (3d, $^1J_{CH}$ = 172 Hz, Tp′*C*H), 120.8, 124.0, 129.3 (3d, $^1J_{CH}$ = 162 Hz, $P(OPh)_3$ C_{ortho},C_{para},C_{meta}), 144.5, 144.6, 146.0, 152.4, 154.1 (5m, Tp′C—CH_3), 151.9 (d, $^2J_{CP}$ = 11 Hz, $P(OPh)_3C_{ipso}$), 233.7 (br s, *CO*), 261.4 (d, $^2J_{CP}$ = 50 Hz, —*C*(O)CH_3); $^{31}P\{^1H\}$ NMR (CD_2Cl_2) δ 164.4 (s). Calcd: C, 55.84; H, 5.17; N, 10.85. Obsd: C, 55.53; H, 5.23; N, 10.24.

$Tp'(CO)(P(OPh)_3)MoC(O)Et$ (4b) (70% yield after chromatography): IR (KBr) ν_{BH} 2532 w, ν_{CO} 1797 s, ν_{CC} 1586 m, ν_{CN} 1544 w; ^1H NMR (CD_2Cl_2) δ 1.62 (t, $^3J_{HH}$ = 8 Hz, 3 H, —CH_2CH_3), 4.04, 4.31 (each a m, each 1 H, —CH_2CH_3); $^{13}C\{^1H\}$ NMR (CD_2Cl_2) δ 233.8 (d, $^2J_{CP}$ = 14 Hz, *CO*), 263.9 (d, $^2J_{CP}$ = 51 Hz, —*C*(O)CH_2—); $^{31}P\{^1H\}$ NMR (THF/10% C_6D_6) δ 167.5 (s).

$Tp'(CO)(P(OMe)_3)MoC(O)Et$ (5) (70% yield after chromatography): IR (KBr) ν_{BH} 2518 w, ν_{CO} 1798 s, ν_{CN} 1545 m; ^1H NMR (CD_2Cl_2) δ 1.42 (t, $^3J_{HH}$ = 7.4 Hz, 3 H, —CH_2CH_3), 3.36 (d, $^3J_{HP}$ = 10.7 Hz, 9 H, $P(OCH_3)_3$), 3.68 (q, $^3J_{HH}$ = 7.4 Hz, 2 H, —CH_2CH_3); ^{13}C NMR (CD_2Cl_2) 51.0 (qd, $^1J_{CH}$ = 146 Hz, $^2J_{CP}$ = 3 Hz, $P(OCH_3)_3$), 236.8 (d, $^2J_{CP}$ = 14 Hz, *CO*), 269.6 (d, $^2J_{CP}$ = 47 Hz, —*C*(O)CH_2—); $^{31}P\{^1H\}$ NMR (CH_2Cl_2/25% C_6D_6) δ 183.0 (s).

$Tp'(CO)(P(OEt)_3)MoC(O)Et$ (6) (60% yield after chromatography): IR (KBr) ν_{BH} 2528 w, ν_{CO} 1792 s, ν_{CN} 1541 vw; ^1H NMR (CD_2Cl_2) δ 1.15 (td, $^3J_{HH}$ = 6.9 Hz, $^4J_{HP}$ = 1.3 Hz, 9 H, $P(OCH_2CH_3)_3$), 1.36 (dt, $^3J_{HH}$ = 7.6 Hz, $^5J_{HP}$ = 1.0 Hz, 3 H, —C(O)CH_2CH_3), 3.43–3.80 (m, 8 H, $P(OCH_2CH_3)_3$ and —C(O)CH_2CH_3); ^{13}C NMR (CD_2Cl_2) 237.1 (d, $^2J_{CP}$ = 15 Hz, *CO*), 270.3 (dt, $^2J_{CH}$ = 5 Hz, $^2J_{CP}$ = 46 Hz, *C*(O)-CH_2); $^{31}P\{^1H\}$ NMR (CD_2Cl_2) δ 178.7 (s).

$K[Tp'(CO)(L)MoC(O){=}CHR]$ [L = CO, R = H, 7; L = $P(OPh)_3$, R = Me, 8]. (1) IR Spectra. A solution of the acyl complex in THF was transferred by cannula to a flask containing excess (≥10 equiv) KH. The suspension was stirred until the orange-red color of the acyl was replaced with the golden-green color of the enolate. The excess KH was allowed to settle, and the IR sample was then withdrawn from the supernatant. The solution IR spectrum was recorded immediately after transfer to the cell.

(2) NMR Spectra. About 0.2 mmol of the acyl complex and 10–15 equiv of KH were loaded in a 5 mm NMR tube mounted on a glass adapter with a stopcock in the drybox. Then 1 g of THF-d_8 was added. When gas evolution ceased, the stopcock was closed, the sample was removed from the drybox and frozen in liquid nitrogen, and the tube was flame sealed. The sample was centrifuged to precipitate excess KH prior to recording the NMR spectra.

$K[Tp'(CO)_2MoC(O){=}CH_2]$ (7): IR (THF) ν_{CO} 1913 s, 1726 vs, ν_{CN} 1540 w; ^1H NMR (THF-d_8) δ 2.29, 2.38, 2.39, 2.40 (4s, 6:6:3:3 H, Tp′CH_3), 3.91, 4.21 (2s, each 1 H, —C(O)=CH_2), 5.65, 5.72 (2s, 2:1 H, Tp′C—*H*); ^{13}C NMR (THF-d_8) δ 12.7, 13.2, 15.0, 15.9 (4q, Tp′CH_3), 56.7 (dd, $^1J_{CH}$ = 150, 166 Hz, —C(O)=CH_2), 106.2, 106.4 (2d, $^1J_{CH}$ = 170 Hz, Tp′*C*—H), 143.1, 144.5, 151.9, 152.3 (4m, Tp′*C*—CH_3),

(36) Wiley, R. H.; Hexner, P. E. In *Organic Synthesis*; Wiley: New York, 1963; Collect. Vol. IV, pp 351–353.

(37) Trofimenko, S. *J. Am. Chem. Soc.* **1967**, *89*, 6288–6294.

188.3 (s, —C(O)=CH_2), 234.4 (s, CO).

K[Tp′(CO)(P(OPh)$_3$)MoC(O)=CHCH$_3$] (8): ^{1}H NMR (THF-d_8) δ 2.03 (d, $^3J_{HH}$ = 6.3 Hz, 3 H, =CHCH_3), 2.07, 2.28, 2.30, 2.45, 2.48 (5s, 6:3:3:3:3 H, Tp′CH_3), 4.67 (qd, $^3J_{HH}$ = 6.3 Hz, $^4J_{HP}$ = 1.7 Hz, ^{1}H, =CHCH$_3$), 4.91, 5.58, 5.68 (3s, each 1 H, Tp′ C—H), 6.71–6.98 (m, 15 H, P(OC$_6$H$_5$)$_3$); ^{13}C{^{1}H} NMR (THF-d_8) δ 12.9, 13.0, 13.5, 14.6, 15.1, 16.2, 17.1 (7q, Tp′CH_3 and =CHCH_3), 73.6 (signal partially obscured by solvent, =CHCH$_3$), 105.8, 107.3 (2d, $^1J_{CH}$ = 167 Hz, Tp′ C—H), 121.9, 123.0, 130.0 (3d, $^1J_{CH}$ = 160 Hz, P(OPh)$_3$ C_{ortho},C_{meta},C_{para}), 142.8, 142.9, 144.2, 151.0, 152.1, 153.8 (6m, Tp′C—CH$_3$), 154.1 (d, $^2J_{CP}$ = 11 Hz, P(OPh)$_3$ C_{ipso}), 185.2 (d, $^2J_{CP}$ = 51 Hz, —C(O)=C), 200.4 (d, $^2J_{CP}$ = 14 Hz, CO); ^{31}P{^{1}H} NMR (THF-d_8) δ 169.8 (s).

Tp′(CO)$_2$MoC(O)R [R = CMe$_3$, 9; R = CH(CH$_3$)CH$_2$Ph, 10; R = CH(CH$_3$)Si(CH$_3$)$_3$, 11], Tp′(CO)$_2$MoC(O)CMe$_3$ (9). Tp′(CO)$_2$MoC(O)Me (**2a**) (0.75 g, 1.5 mmol) was dissolved in THF and transferred to a Schlenk flask containing excess KH in mineral oil. After hydrogen evolution subsided, the yellow-green enolate solution was transferred (not filtered) to a flask containing 10 equivalents of MeI. The solution immediately turned dark red-brown. After stirring 30 min the solution was filtered, stripped to a brown oil, and redissolved in a minimum amount of benzene. Chromatography on alumina with hexanes/5% diethyl ether eluent provided a single orange-red fraction. Recrystallization from hot heptane yielded orange microcrystalline **Tp′(CO)$_2$MoC(O)CMe$_3$ (9**, 30%): IR (KBr) ν_{BH} 2528 w, ν_{CO} 1947 s, 1846 vs, ν_{CN} 1545 m; ^{1}H NMR (C_6D_6) δ 1.61 (s, 9 H, C(CH_3)$_3$); ^{13}C NMR (C_6D_6) 27.6 (q, $^1J_{CH}$ = 127 Hz, C(CH_3)$_3$, 47.5 (m, $^2J_{CH}$ = 5 Hz, C(CH$_3$)$_3$), 235.2 (s, CO), 250.8 (s, C(O)CMe$_3$). Calcd: C, 49.46; H, 5.85; N, 15.73. Obsd: C, 49.34; H, 5.90; N, 16.35.

Tp′(CO)$_2$MoC(O)R [R = CH(CH$_3$)CH$_2$Ph, 10]. Aliquots of n-BuLi in hexanes were added by syringe to Tp′(CO)$_2$MoC(O)Et (**2b**, 1.14 g, 2.30 mmol) in 120 mL of THF at −78 °C until the characteristic gold color of the enolate was observed. The enolate solution was transferred by cannula to a flask containing benzyl bromide (2.7 mL, 23 mmol). After removal of THF, the excess benzyl bromide was distilled away from the deep red-purple oil at 80–100 °C under vacuum. Chromatography on alumina (hexanes/5% diethyl ether eluent) afforded Tp′(CO)$_2$MoC(O)CH(CH$_3$)CH$_2$Ph (**10**) as a reddish-orange powder (1.30 g, 2.19 mmol, 95%), which was then recrystallized in hot heptane to give dark red microcrystals. **Tp′(CO)$_2$MoC(O)CH(CH$_3$)CH$_2$Ph (10)**: IR (KBr) ν_{BH} 2524 w, ν_{CO} 1958 s, 1828 vs, ν_{CN} 1542 m; ^{1}H NMR (C_6D_6) δ 1.43 (d, $^3J_{HH}$ = 7.0 Hz, 3 H, —CHCH_3), 2.89 (dd, $^2J_{HH}$ = 13.2 Hz, $^3J_{HH}$ = 10.7 Hz, 1 H, —CHMeCH^aH^bPh), 3.77 (dd, $^2J_{HH}$ = 13.2 Hz, $^3J_{HH}$ = 4.5 Hz, 1 H, —CHMeCH^aH^bPh), 4.38 (m, 1 H, —CH(CH$_3$)CH$_2$—); ^{13}C{^{1}H} NMR (C_6D_6) δ 233.1 (s, CO), 251.7 (s, C(O)CH—). Calcd: C, 54.47; H, 5.59; N, 14.12. Obsd: C, 54.29, H, 5.70; N, 14.01.

Tp′(CO)$_2$MoC(O)CH(CH$_3$)Si(CH$_3$)$_3$ (11). This compound was prepared as described for Tp′(CO)$_2$MoC(O)CH(CH$_3$)CH$_2$Ph (**10**) using Me$_3$SiCl in place of PhCH$_2$Br. The crude orange product was extracted into warm methylbutane, filtered, reduced in volume, and cooled slowly, giving Tp′(CO)$_2$MoC(O)CH(CH$_3$)Si(CH$_3$)$_3$ (**11**) as a bright orange powder (94% yield after recrystallization). This product is hygroscopic: IR (THF) ν_{CO} 1960 s, 1853 vs, ν_{CN} 1545 m; ^{1}H NMR (CD_2Cl_2) δ 0.44 (s, 9 H, —Si(CH_3)$_3$), 1.63 (d, $^3J_{HH}$ = 6.6 Hz, 3 H, —CH(CH$_3$)—), 4.16 (q, $^3J_{HH}$ = 6.6 Hz, 1 H, —CH(CH$_3$)—); ^{13}C{^{1}H} NMR (CD_2Cl_2) δ −1.75 (Si(CH_3)$_3$), 236.0, 236.6 (CO), 256.8 (—C(O)CH—). Calcd: C, 47.78; H, 6.05; N, 14.53. Obsd: C, 47.76; H, 6.21; N, 13.85.

Tp′(CO)(P(OPh)$_3$)MoC(O)CH$_2$CH$_2$Ph. The enolate of Tp′(CO)(P(OPh)$_3$)MoC(O)Me (**4a**) was alkylated with PhCH$_2$Br as described for the preparation of Tp′(CO)$_2$MoC(O)CH(CH$_3$)CH$_2$Ph (**10**). Chromatography on alumina with benzene/5% diethyl ether eluent gave Tp′(CO)(P(OPh)$_3$)MoC(O)CH$_2$CH$_2$Ph as an orange powder (59% yield): IR (THF) ν_{CO} 1814 s, ν_{CC} 1586 m; ^{1}H NMR (CD_2Cl_2) δ 1.76, 2.02, 2.31, 2.44 (each a s, 3:6:6:3 H, Tp′CH_3), 3.26, 3.48, 4.16, 4.64 (each a br m, each 1 H, —C(O)(CH_2)$_2$Ph), 5.16, 5.82, 5.88 (each a s, each 1 H, Tp′C—H), 6.6–7.5 (m, 15 H, P(OC$_6$H$_5$)$_3$).

Preparation of Mixtures of Diastereomers: Tp′(CO)(L)MoC(O)CH(CH$_3$)CH$_2$Ph [L = P(OPh)$_3$, 12,12′; L = P(OMe)$_3$, 24,24′; L = P(OEt)$_3$, 25,25′]. Mixtures of diastereomers were prepared by photolysis of the corresponding dicarbonyl complex in CH$_3$CN followed by treatment with the appropriate phosphite. Chromatography on alumina followed by trituration with methylbutane afforded a mixture of both diastereomers. Tp′(OC)(P(OPh)$_3$)MoC(O)CH(CH$_3$)CH$_2$Ph (12,12′) (12:12′ ≈ 80:20 after chromatography, determined by ^{1}H NMR), **12** (major isomer): IR (KBr) ν_{BH} 2520 vw, ν_{CO} 1816 s, ν_{CC} 1587 m, ν_{CN} 1542 w; ^{1}H NMR (CD_2Cl_2) δ 1.48 (d, $^3J_{HH}$ = 6.9 Hz, 3 H, —CH(CH_3)—), 2.75 (dd, $^2J_{HH}$ = 13.3Hz, $^3J_{HH}$ = 10.8 Hz, 1 H, —CHMeCH^aH^bPh), 4.19 (dd, $^1J_{HH}$ = 13.3 Hz, $^3J_{HH}$ = 2.4 Hz, 1 H, —CHMeCH^aH^bPh), 5.3 (m, 1 H, —CH(CH$_3$)CH$_2$—); ^{13}C NMR (CD_2Cl_2) δ 39.2 (t, $^1J_{CH}$ = 136 Hz, —CHCH$_2$Ph), 49.1 (d, $^1J_{CH}$ = 137 Hz, —CH(CH$_3$)CH$_2$—), 234.7 (d, $^2J_{CP}$ = 13 Hz, CO), 262.9 (d, $^2J_{CP}$ = 51 Hz, —C(O)CH)—; ^{31}P{^{1}H} NMR (CD_2Cl_2) 166.2 (s); Calcd for $C_{45}H_{50}BMoN_6O_{5.25}P$ (MW 896.66, 0.25 THF solvate/molecule determined by ^{1}H NMR): C, 60.28; H, 5.62; N, 9.37. Obsd: C, 60.26; H, 5.80; N, 9.11. **12′** (minor isomer): IR (KBr) ν_{BH} 2520 vw, ν_{CO} 1816 s, ν_{CC} 1587 m, ν_{CN} 1542 w; ^{1}H NMR (CD_2Cl_2) δ 1.72 (d, $^3J_{HH}$ = 7.3 Hz, 3 H, —CH(CH_3)—), 3.08 (dd, $^2J_{HH}$ = 13.7 Hz, $^3J_{HH}$ = 9.6 Hz, 1 H, —CHMeCH^aH^bPh), 3.50 (dd, $^2J_{HH}$ = 13.7 Hz, $^3J_{HH}$ = 3.1 Hz, 1 H, —CHMeCH^aH^bPh), 5.2 (m, 1 H, —CH(CH$_3$)CH$_2$—); ^{13}C NMR (CD_2Cl_2) δ 40.0 (t, $^1J_{CH}$ = 129 Hz, —CHCH$_2$Ph), 49.4 (d, $^1J_{CH}$ = 134 Hz, —CH(CH$_3$)CH$_2$—), 234.7 (d, $^2J_{CP}$ = 13 Hz, CO), 263.9 (d, $^2J_{CP}$ = 53 Hz, —C(O)CH—); ^{31}P{^{1}H} NMR (CD_2C_{12}) δ 166.8 (s).

Tp′(CO)(P(OMe)$_3$)MoC(O)CH(CH$_3$)CH$_2$Ph (24,24′) (24:24′ ≈ 65:35 after chromatography, determined by ^{1}H NMR), **24** (major isomer): IR (KBr) ν_{BH} 2532 vs, ν_{CO} 1804 s, ν_{CN} 1543 w; ^{1}H NMR (CD_2Cl_2) δ 1.18 (d, $^3J_{HH}$ = 6.6 Hz, 3 H, —CH(CH_3)—), 1.92–2.50 (—CHMeCH^aH^b and Tp′CH_3), 3.33 (d, $^3J_{PH}$ = 9.5 Hz, 9 H, P(OCH_3)$_3$), 3.85 (dd, $^2J_{HH}$ = 13.3 Hz, $^3J_{HH}$ = 3.0 Hz, 1 H, —CHMeCH^aH^b), 4.56 (v. br, —CH(CH$_3$)CH$_2$—); ^{13}C NMR (CD_2Cl_2) δ 38.8 (t, $^1J_{CH}$ = 130 Hz, —CHCH$_2$Ph), 51.4 (q, $^1J_{CH}$ = 164 Hz, P(OCH$_3$)$_3$), 237.0 (br s, CO), 268.1 (br s, —C(O)CH—); ^{31}P{^{1}H} NMR (CH_2Cl_2/25% C_6D_6) δ 176.4 (br s). **24′** (minor isomer): IR (KBr) ν_{BH} 2532 vw, ν_{CO} 1804 s, ν_{CN} 1543 w; ^{1}H NMR (CD_2Cl_2) δ 1.35 (d, $^3J_{HH}$ = 6.9 Hz, 3 H, —CH(CH_3)—), 2.75 (dd, $^2J_{HH}$ = 13.7, $^3J_{HH}$ = 10.5 Hz, 1 H, —CHCH^aH^b—), ~3.25 (dd, partially obscured by P(OCH_3)$_3$, $^3J_{HH}$ = 3.3 Hz, —CHCH^aH^b—), 3.31 (d, $^3J_{PH}$ = 9.4 Hz, 9 H, P(OCH_3)$_3$), 4.56 (v. br s, —CH(CH$_3$)CH$_2$—); ^{31}P{^{1}H} NMR (CH_2Cl_2/25% C_6D_6) δ 176.7 (br s).

Tp′(CO)(P(OEt)$_3$)MoC(O)CH(CH$_3$)CH$_2$Ph (25,25′) (25:25′ = 60:40, determined by ^{31}P{^{1}H} NMR of crude product), **25** (major isomer in crude product mixture): ^{31}P{^{1}H} NMR (CH_2Cl_2/CD_2Cl_2) δ 174.9 (s). **25′** (minor isomer in crude product mixture, isolated by chromatography on alumina): ν_{BH} 2520 w, ν_{CO} 1795 s, ν_{CN} 1544 m; ^{1}H NMR (C_6D_6) δ 1.44 (d, $^3J_{HH}$ = 6.7 Hz, 3 H, —CH(CH_3)—), 2.81 (dd, $^2J_{HH}$ = 13.8 Hz, $^3J_{HH}$ = 11.7 Hz, 1 H, —CHMeCH^aH^bPh), 4.30 (dd, $^2J_{HH}$ = 13.8 Hz, $^3J_{HH}$ = 2.9 Hz, 1 H, —CHMeCH^aH^bPh), 4.83 (m, 1 H, —CH(CH$_3$)CH$_2$—); ^{13}C NMR (CD_2Cl_2) δ 38.8 (t, $^1J_{CH}$ = 130 Hz, —CHCH$_2$Ph), 49.3 (d, $^1J_{CH}$ = 136 Hz, —CH(CH$_3$)CH$_2$—), 236.7 (d, $^2J_{CP}$ = 16 Hz, CO), 268.4 (d, $^2J_{CP}$ = 48 Hz, —C(O)CH—); ^{31}P NMR (CH_2Cl_2/CD_2Cl_2) δ 172.6 (s).

Phosphite Exchange NMR Experiment: Tp′(CO)[P(OPh)$_3$]MoC(O)Et + P(OEt)$_3$ and Tp′(CO)[P(OEt)$_3$]MoC(O)Et + P(OPh)$_3$. A 10-mm NMR tube was charged with 0.20 mmol of the phosphite-substituted acyl complex, ca. 1 equiv of the liquid phosphite, and 4 mL of tetrahydrofuran/10% C_6D_6. The sample was frozen in liquid nitrogen and sealed under vacuum. Both exchange reactions were monitored by ^{31}P NMR at 30-min intervals for the first 2 h and then at 24-h intervals. **Tp′(CO)(P(OPh)$_3$)MoC(O)Et (4b)**: ^{31}P{^{1}H} NMR (THF/10% C_6D_6) δ 167.3. **Tp′(CO)(P(OEt)$_3$)MoC(O)Et (6)**: ^{31}P{^{1}H} NMR (THF/10% C_6D_6) δ 179.1. **P(OPh)$_3$**: ^{31}P{^{1}H} NMR (THF/10% C_6D_6) δ 128.4. **P(OEt)$_3$**: ^{31}P{^{1}H} NMR (THF/10% C_6D_6): δ 183.2. All four signals were uniform in shape, and the extent of phosphite exchange was based on the integrated intensities of the ^{31}P NMR signals.

Diastereoselectivity Assays. To a solution of Tp′(CO)(L)MoC(O)R (ca. 0.35 mmol for L = P(OPh)$_3$, ca. 0.10 mmol for L = P(OMe)$_3$) in THF at −78 °C was added n-BuLi (1 equiv, 2.6 M in hexanes). After stirring at −78 °C for a few minutes the enolate solution was transferred to a flask containing 10–15 equivalents of the halide reagent. After stirring 30 min at room temperature, the THF was evaporated to leave a red paste. When L = P(OPh)$_3$, the crude product was dissolved in 4 mL of CH_2Cl_2/10% C_6D_6, transferred to a 10-mm NMR tube, and the ^{31}P{^{1}H} NMR spectrum was taken. Product ratios were calculated from the integrated peak intensities of the two products. The P(OMe)$_3$ derivatives were dissolved in CD_2Cl_2 and transferred to 5-mm NMR tubes. Diastereomer ratios were determined from the integrated phosphite ^{1}H methyl doublets near 3.3 ppm.

Tp′(CO)$_2$MoC(O)C(R)=CR′Ph [R = H, R′ = H, 13; R = H, R′ = Ph, 14; R = Me, R′ = H, 15]. In a representative synthesis, 1 equiv of n-BuLi in hexanes was added to a solution of Tp′(CO)$_2$MoC(O)Me (**2a**, 7.38 g, 15.0 mmol) in THF (200 mL) at −78 °C. The resultant orange-brown enolate solution was transferred by cannula to a flask containing neat PhCHO (3.8 mL, 37.5 mmol). Within seconds the mixture began to turn deep indigo. After stirring 30 min, 1 mL of acid (H_2O + 2 drops HCl) was added. The dark solution was stirred overnight, and then evaporation of solvent gave a purple paste which was dissolved in CH_2Cl_2 (250 mL) and filtered through a 5 × 8 cm column of alumina, using CH_2Cl_2 as eluent. The indigo material was collected, stripped to a paste, triturated with methylbutane, and dried to give Tp′(CO)$_2$MoC(O)CH=CHPh (**13**) (6.23 g, 10.7 mmol, 72%). **Tp′(CO)$_2$MoC(O)CH=CHPh (13)**: IR (KBr) ν_{BH} 2520 vw, ν_{CO} 1943 s, 1836 vs, ν_{CC} 1596 w, ν_{CN} 1543 w; ^{1}H NMR (CD_2Cl_2) 2.07, 2.31, 2.42, 2.45 (4s, 6:3:6:3 H,

Tp'CH_3), 5.85, 5.92 (2s, 2:1 H, Tp'C—H), 7.57, 7.81 (2d, $^3J_{HH}$ = 15.7 Hz, each 1 H, —CH=CHPh), 7.48–7.50, 7.75–7.76 (m, 3:2 H, C_6H_5); ^{13}C NMR (CD_2Cl_2/12% $(CH_3)_2CO$) δ 11.2, 12.6, 13.4, 14.2, 15.4 (5q, Tp'CH$_3$), 106.8, 107.5 (2d, $^1J_{CH}$ = 175 Hz, Tp'C—H), 117.8 (d, $^1J_{CH}$ = 164 Hz, —C(O)CH=CHPh), 129.2, 129.5, 131.4 (3d, $^2J_{CH}$ = 150–160 Hz, Ph C_{ortho},C_{meta}, and C_{para}), 135.2 (s, Ph C_{ipso}), 146.3 (d, $^1J_{CH}$ = 164 Hz —CH=CHPh), 144.9, 147.0, 151.8, 152.8 (4m, Tp'C—CH_3), 233.1 (s, CO), 237.1 (s, C(O)CH=). Calcd: C, 53.84; H, 5.00; N, 14.49. Obsd: C, 53.45; H, 5.19; N, 14.20.

$Tp'(CO)_2MoC(O)CH{=}CPh_2$ (14) (76% yield after chromatography): IR (THF) ν_{CO} 1948 s, 1853 vs; ^{1}H NMR (CD_2Cl_2) δ 7.91 (s, 1 H, —CH=CPh_2); ^{13}C NMR (CD_2Cl_2) δ 116.4 (d, $^1J_{CH}$ = 165 Hz, —C(O)CH=), 152.3 (s, —CH=CPh$_2$), 233.2 (s, CO), 234.1 (d, $^2J_{CH}$ = 5 Hz, —C(O)CH=).

$Tp'(CO)_2MoC(O)C(CH_3){=}CHPh$ (15): (60–70% yield after chromatography): IR (KBr) ν_{CO} 1943 s, 1846 vs, ν_{CC} 1608 vw, ν_{CN} 1541 w; ^{1}H NMR (CD_2Cl_2) δ 2.62 (d, $^4J_{HH}$ = 1.2 Hz, 3 H, —C(CH_3)=CHPh), 7.99 (q, $^4J_{HH}$ = 1.2 Hz, 1 H, —(CH_3)=CHPh); ^{13}C NMR (CD_2Cl_2) δ 16.9 (dq, $^1J_{CH}$ = 128 Hz, $^3J_{CH}$ = 9 Hz, —C(CH_3)=CHPh), 130.0 (q, $^2J_{CH}$ = 8 Hz, —C(O)C(CH_3)=), 148.9 (dq, $^1J_{CH}$ = 159 Hz, $^3J_{CH}$ = 4 Hz, —C(CH_3)=CHPh), 234.1 (s, CO), 238.5 (m, —C(O)C(CH_3)=). Calcd: C, 54.59; H, 5.22; N, 14.15. Obsd: C, 54.47; H, 5.00; N, 14.47.

$Tp'(CO)_2Mo(\eta^3\text{-}CH_2CHCHPh)$ (17). A solution of $Tp'(CO)_2MoC(O)C(CH_3){=}CHPh$ (**15**) (0.89 g, 1.5 mmol) in toluene (90 mL) was refluxed under nitrogen for 4 days. The red-brown solution was then stripped to a powder which was dissolved in benzene and filtered through alumina. Solvent removal and recrystallization from THF/Et_2O/hexanes gave cranberry red needles of **17** (0.75 g, 1.32 mmol, 88%): IR (KBr) ν_{BH} 2522 w, ν_{CO} 1927 vs, 1817 vs, ν_{CN} 1543 m; ^{1}H NMR (CD_2Cl_2) δ 2.06 (dd, $^3J_{HaHc}$ = 10.3 Hz, $^2J_{HaHs}$ = 1 Hz, 1 H, allyl Ha), 2.23, 2.25, 2.28, 2.32, 2.42, 2.45 (6s, each 3 H, Tp'CH_3), 3.67 (dd, $^3J_{HsHc}$ = 6.8 Hz, $^2J_{HaHs}$ = 1 Hz, 1 H, allyl Hs), 4.22 (d, $^3J_{Ha'Hc}$ = 9.8 Hz, 1 H, allyl Ha'), 5.37 (m, 1 H, allyl Hc), 5.51, 5.87, 5.83 (3s, each 1 H, Tp' C—H), 6.90–6.98, 7.04–7.10 (each a m, 2:3 H, —C_6H_5); ^{13}C NMR (CD_2Cl_2) δ 57.8 (t, $^1J_{CH}$ = 160 Hz, allyl Ca), 83.1 (d, $^1J_{CH}$ = 165 Hz, allyl Cc), 90.2 (d, $^1J_{CH}$ = 166 Hz, allyl Cb), 230.5, 235.1 (2s, CO). Calcd: C, 55.17; H, 5.48; N, 14.85. Obsd: C, 55.10; H, 5.81; N, 15.09.

Conjugate Additions to Dicarbonyl η^2-Enone Complexes. (1) $NaBH_4/H_3O^+$. To a solution of $Tp'(CO)_2MoC(O)CH{=}CHPh$ (**13**) (0.28 g, 0.48 mmol) in THF/50% MeOH (50 mL) at 0 °C was added $NaBH_4$ (0.16 g, 4.2 mmol). The solution was stirred for 2 h at room temperature before aqueous acid (2 mL of H_2O + 3 drops of HCl) was added. The reaction mixture was stripped to an olive green solid, dissolved in benzene (10 mL), and chromatographed on alumina. The orange product was eluted with hexanes/40% benzene, while a small amount of indigo starting material remained on the column. Evaporation of the solvent yielded $Tp'(CO)_2MoC(O)CH_2CH_2Ph$ (**18**) (0.21 g, 0.36 mmol, 75%) as a light orange powder which was then crystallized from hot hexanes: IR (KBr) ν_{BH} 2520 vw, ν_{CO} 1964s, 1834 vs, ν_{CN} 1543 m; ^{1}H NMR ($CDCl_3$) 3.29, 4.03 (each a t, $^3J_{HH}$ = 7.8 Hz, each 2 H, —CH_2CH_2—). Calcd: C, 53.65; H, 5.33; N, 14.44. Obsd: C, 53.92; H, 5.42; N, 14.24.

(2) $K[HB(OPr^i)_3]$/MeI. To a solution of $Tp'(CO)_2MoC(O)CH{=}CHPh$ (**13**) (0.63 g, 1.09 mmol) in THF (65 mL) was added $K[HB(OPr^i)_3]$ (2 equiv, 1 M in THF). The solution was heated at 40–50 °C for 1.5 h, resulting in a golden brown solution with ν_{CO} 1912, 1723 cm^{-1}. Addition of excess MeI at −42 °C resulted in a red-orange solution as KI precipitated. Solvent evaporation left an orange powder which was dissolved in benzene (10 mL) and chromatographed on alumina. Elution with hexanes/30% benzene gave $Tp'(CO)_2MoC(O)CH(CH_3)CH_2Ph$ (**19**) (0.58 g, 0.97 mmol, 89%). IR and ^{1}H NMR spectra of **19** prepared in this manner were identical with spectra of a sample prepared by benzylation of $Li[Tp'(CO)_2MoC(O)CHCH_3]$ (see **10** above).

(3) $MeLi/H_3O^+$. MeLi (1.6 equiv, 1.4 M in Et_2O) was added in aliquots to a cold THF solution (−42 °C) containing 1.03 g of $Tp'(CO)_2MoC(O)CH{=}CHPh$. After stirring for 10 m the solution was allowed to warm to room temperature, and 10 mL of 0.5 M aqueous HCl was added. The solution was stirred overnight and stripped to a paste, and the residue was dissolved in benzene. Two phases resulted; the upper benzene solution was transferred to a 2.5 × 5 cm alumina column, and the lower aqueous layer was discarded. Hexanes/benzene (60/40) eluted the orange product. Evaporation of the solvent and recrystallization from hot hexane yielded pure $Tp'(CO)_2MoC(O)CH_2CHMePh$ (**20**) (0.28 g, 0.47 mmol, 27%): IR (KBr) 1950, 1850 cm^{-1}. Calcd: C, 54.38; H, 5.54: N, 14.10. Obsd: C, 54.53; H, 5.89; N, 13.98.

(4) MeLi/MeI. MeLi (1.5 equiv, 1.4 M in Et_2O) was added in aliquots to a solution of $Tp'(CO)_2MoC(O)C(CH_3){=}CHPh$ (**15**) in distilled THF at −42 °C. After stirring 10 min an excess of MeI was added to the forest green reaction mixture. The solution turned orange-red within minutes. The solvent was removed, and the crude product was dissolved in benzene and chromatographed on alumina. Recrystallization from hot heptane gave red crystals of $Tp'(CO)_2MoC(O)C(CH_3)_2CH(CH_3)Ph$ (**21**) (62% yield): IR (KBr) ν_{BH} 2525 vw, ν_{CO} 1943 s, 1845 s, ν_{CN} 1545 w; ^{1}H NMR (C_6D_6) δ 1.48 (s, 3 H, —C(O)C(CH_3)—), 1.61 (d, $^3J_{HH}$ = 7.0 Hz, 3 H, —CH(CH_3)Ph), 3.73 (q, $^3J_{HH}$ = 7.0 Hz, 1 H, —CH(CH_3)Ph); ^{13}C NMR (C_6D_6) δ 26.7 (q, $^1J_{CH}$ = 128 Hz, —C(O)C(CH_3)—), 47.8 (d, $^1J_{CH}$ = 130 Hz, —CH(CH_3)Ph), 55.1 (s, —C(O)C(CH_3)$_2$—), 235.1, 237.5 (2s, CO), 252.4 (s, C(O)C(CH_3)$_2$—).

$Tp'(CO)_2Mo\overline{C(R)C(R)C(O)}Et$ [R = Et, 22; R = Ph, 23]. In a representative synthesis, a CH_3CN solution of $Tp'(CO)_2MoC(O)Et$ (**2b**) (2.67 g, 5.27 mmol) was photolyzed at 0 °C until the reaction was about 80% complete by IR (3 h). Removal of the solvent gave a red-brown oil which was then dissolved in CH_2Cl_2 (70 mL) and cooled to 0 °C. 3-Hexyne (1.32 mL, 11.6 mmol) was added, and the reaction mixture was stirred at 0 °C for 30 min and was then warmed to 40 °C for 30 min. The IR of the golden brown solution indicated complete consumption of the acetonitrile adduct and formation of a monocarbonyl intermediate (ν_{CO} = 1851 cm^{-1}). The reaction flask was evacuated and filled with carbon monoxide gas three times and then stirred under CO overnight. Evaporation of the solvent gave a brown oil which was dissolved in benzene and chromatographed on alumina. Hexanes/30% benzene was used to elute the bright yellow product $Tp'(CO)_2Mo\overline{C(Et)C(Et)C(O)}Et$ (**22**), which was then stripped to a yellow powder (0.49 g, 0.83 mmol, 16%). Solutions of **22** are light sensitive and turn green in about 30 min of exposure to room light.

$Tp'(CO)_2Mo\overline{C(Et)C(Et)C(O)}Et$ (22): IR (KBr) ν_{BH} 2528 vw, ν_{CO} 1947 vs, 1863 vs, ν_{CN} 1545 w; ^{1}H NMR (CD_2Cl_2) δ 1.17, 1.23, 1.57 (3t, $^3J_{HH}$ = 7.5 Hz, each 3 H, —CH_2CH_3), 1.68, 2.48, 2.54 (3s, 6:9:3 H, Tp' CH_3), 2.71, 2.72, 3.98 (3q, $^3J_{HH}$ = 7.5 Hz, each 2 H, —CH$_2$CH$_3$), 5.88, 6.01 (2s, 2:1 H, Tp' C—H); ^{13}C NMR (CD_2Cl_2) δ 12.6, 12.8, 13.4, 13.6,

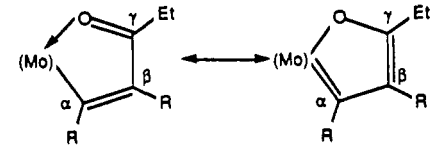

15.5, 16.6 (6q, —CH_2CH_3 and Tp'CH$_3$), 22.7, 28.7, 43.4 (3tq, $^1J_{CH}$ = 127 Hz, $^2J_{CH}$ = 4 Hz, —CH$_2$CH$_3$), 106.7, 108.1 (2d, $^1J_{CH}$ = 175 Hz, Tp' C—H), 135.1 (s, C_β), 144.9, 146.6, 151.6, 153.2 (4m, Tp'C—CH_3), 191.9 (s, C_γ), 243.9 (s, CO), 252.6 (s, C_α).

$Tp'(CO)_2Mo\overline{C(Ph)C(Ph)C(O)}Et$ (23) (40% yield after chromatography). Like compound **22** the diphenyl derivative **23** is bright yellow, but solutions gradually turn emerald green. Solids and solutions of **23** which are kept in the dark remain yellow-orange indefinitely: IR (KBr) ν_{BH} 2535 vw, ν_{CO} 1965 vs, 1873 vs, ν_{CC} 1597 vw, ν_{CN} 1545 w; ^{1}H NMR (CD_2Cl_2) δ 1.13 (t, $^3J_{HH}$ = 7.6 Hz, 3 H, —CH_2CH_3), 2.69 (q, $^3J_{HH}$ = 7.6 Hz, 2 H, —CH_2CH$_3$); ^{13}C NMR (CD_2Cl_2) 191.9 (s, C_γ), 244.0 (s, CO), 250.3 (s, C_α).

Structural Determinations of $Tp'(CO)(P(OPh)_3)MoC(O)CH(CH_3)CH_2Ph$ (12), $Tp'(CO)_2MoC(O)CH{=}CPh_2$ (14), and $Tp'(CO)_2Mo\overline{C(Et)C(Et)C(O)}Et$ (22). $Tp'(CO)(P(OPh)_3)MoC(O)CH(CH_3)CH_2Ph$ (**12**) was prepared by treatment of a THF solution of $Li[Tp'(CO)(P(OPh)_3)MoC(O)CHCH_3]$ (**13**) with 15 equiv of $PhCH_2Cl$. The solution was stirred for 30 min, and then THF was removed to leave a concentrated benzyl chloride solution of **12**. Crystals suitable for an X-ray diffraction study formed overnight from this solution. Single crystals of $Tp'(CO)_2MoC(O)CH{=}CPh_2$ (**14**) were obtained by layering hexane over a CH_2Cl_2 solution of **14**. Single crystals of $Tp'(CO)_2Mo\overline{C(Et)C(Et)C(O)}Et$ (**22**) were grown by slow cooling of a heptane solution.

Collection of X-ray Diffraction Data. Diffraction data were collected on an Enraf-Nonius CAD-4 automated diffractometer.[38] Twenty-five reflections located in the region 30° < 2θ < 35° were centered, and angular data were refined by least-squares calculations. The lattice system which was indicated and the associated cell constants are listed in Table VII.

Diffraction data were collected in the hemisphere (+h,±k,±l) under the conditions specified in Table VII. Three reflections chosen as intensity standards were monitored every 3 h and showed no significant (<1.0%) decay. The crystal was checked for orientation after every 300 reflections, and recentering was performed if the scattering vectors varied by more than 0.15°. ψ scans of nine reflections having 80° < χ < 90° were used to calculate an empirical absorption correction. Unique reflections were collected in the region 2° < θ < 25°, and the data were reduced and corrected for Lorentz polarization effects. Only reflections with $I > 3\sigma(I)$ were used in the structure solutions.

Table VII. Crystallographic Data

	Tp′(CO)(P(OPh)$_3$)-MoC(O)CH(CH$_3$)CH$_2$Ph (**12**)	Tp′(CO)$_2$-MoC(O)CH=CPh$_2$ (**14**)	Tp′(CO)$_2$MoC(Et)-C(Et)C(O)Et (**22**)
molecular formula	$C_{44}H_{48}BMoN_6O_5P$	$MoO_3N_6C_{32}H_{33}\cdot{}^1/_2CH_2Cl_2$	$C_{26}H_{37}BMoN_6O_3$
formula wt, g/mol	878.64	688.04	588.37
crystal dimensions, mm	0.45 × 0.40 × 0.42	0.70 × 0.20 × 0.15	0.20 × 0.20 × 0.40
space group	$P\bar{1}$	$P\bar{1}$	$P\bar{1}$
cell dimensions			
a, Å	14.142 (4)	13.789 (4)	13.830 (2)
b, Å	15.625 (4)	10.090 (2)	10.102 (2)
c, Å	11.147 (2)	12.918 (3)	10.527 (4)
α, deg	99.88 (2)	72.04 (2)	78.94 (2)
β, deg	92.23 (2)	103.21 (2)	97.11 (2)
γ, deg	90.50 (2)	92.51 (2)	92.86 (2)
vol, Å^3	2424 (2)	1664 (1)	1432 (1)
z, molecules/cell	2	2	2
ρ calcd, g/cm^3	1.20	1.37	1.36
radiatn (wavelength, Å)	Mo Kα (0.71073)	Mo Kα (0.71073)	Mo Kα (0.71073)
monochromator	graphite	Zr filter	Zr filter
linear abs. coeff, cm^{-1}	3.49	5.13	4.91
scan type	$\omega/1.67\theta$	$\omega/1.33\theta$	$\omega/0.67\theta$
background	25% of full scan width on both sides	25% of full width on both sides	25% of full scan width on both sides
θ limits	$2° < \theta < 20°$	$2° < \theta < 25°$	$2° < \theta < 24°$
hemisphere collected	$+h\pm k\pm l$	$+h\pm k\pm l$	$+h\pm k\pm l$
total no. reflens	4739	6102	4679
data with $I \geq 3\sigma(I)$	3017	3683	3467
R	7.7%	5.6%	3.9%
R_w	6.8%	4.4%	4.3%
GOF	2.56	2.18	1.90
no. of paras	323	328	334
largest parameter shift/esd	0.67	0.04	0.00

Scheme XI

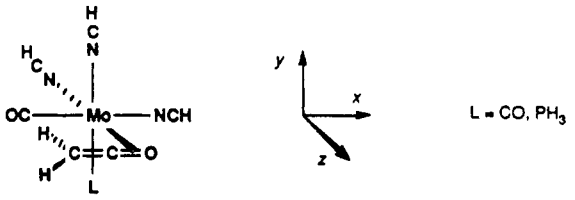

Solution and Refinement of the Structure. Each of the three structure solutions was straightforward from the application of the heavy-atom method. The molybdenum atom was located in the three-dimensional Patterson function. The remaining non-hydrogen atoms were located by subsequent Fourier and difference Fourier calculations. Final agreement indices[39] are indicated in Table VII. For complex **12** the final refinement was with hydrogens placed in calculated positions (d(C–H) = 0.95 Å), the phenyl carbons of the triphenylphosphite and all of the hydridotris(3,5-dimethylpyrazolyl)borate atoms refined isotropically, and the remaining atoms refined anisotropically. For complex **14** the final refinement was with the 12 phenyl carbons refined isotropically and all other non-hydrogen atoms refined anisotropically. For complex **22** the hydrogens were placed in calculated positions (d(C–H) = 0.95 Å), and all other atoms were refined anisotropically.

Extended Hückel Calculations. EHMO calculations were performed with Professor R. Hoffmann's programs ICON8 and FMO employing the weighted H_{ij} option.[40] (HCN)$_3$(CO)(L)MoC(O)=CH$_2$ [L = CO, PH$_3$] was used as a model system. The coordinate systems associated with the model compounds are defined in Scheme XI.

The model complexes were idealized as octahedra, with the ligands in the [(HCN)$_3$(CO)(L)Mo]$^{2+}$ fragment placed on the $\pm x$, $\pm y$, and $-z$ axes. Bond distances for this fragment were obtained from structurally characterized Tp(CO)(L)MoC(O)Me [Tp = hydridotris(pyrazolyl)borate, L = CO, PEt$_3$, P(OMe)$_3$].[12] The enolate moiety was treated as a 2$^-$ fragment. The geometry of the enolate ligand was based on structural parameters reported for [Cp$_2$Zr(CH$_3$)(C(O)=CH$_2$)]$^-$,[18a] with appropriate corrections for the difference in radii of Mo and Zr. Bond distances and angles for the model compounds are collected in Table VIII. The midpoint of the enolate C–O bond was placed on the $+z$ axis with the enolate C–O vector antiparallel to the Mo–CO vector defined as 0°. The enolate fragment was then rotated about the z axis, with positive rotation defined in the counterclockwise direction. Plots of energy versus enolate rotational angle are available as Supplementary Material.

Table VIII. Bond Distances and Angles for Model Compounds

bond	distance (Å)	bond	distance (Å)
	Metal Fragment		
Mo–N	2.10	N–CH	1.16
Mo–CO	2.00	NC–H	1.00
Mo–P	2.53	C–O	1.15
		P–H	1.44
	Enolate Fragment		
Mo–C	2.00	C–O	1.34
Mo–O	2.00	C=C	1.32
		C–H	1.00

Bond Angles

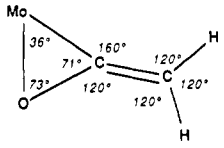

Acknowledgment. We thank the National Science Foundation for support of this work (CHE-8521840). Helpful conversations with Professor M. T. Crimmins and Professor M. S. Brookhart are gratefully acknowledged.

Supplementary Material Available: Complete tables of atomic coordinates, temperature factors, and bond lengths and angles for compounds **12**, **14** and **22**, ν_{CO} vibrational data and ^{1}H and ^{13}C NMR data for all compounds, and rotational energy profiles for EHMO calculations for enolate rotation (41 pages); tables of observed and calculated structure factors for **12**, **14**, and **22** (74 pages). Ordering information is given on any current masthead page.

(38) Programs utilized during data collection and structure solution and refinement were provided by Enraf-Nonius as part of the Structure Determination Package (SCP, 3rd ed., August 1978, revised June 1979.)

(39) The function minimized was $\Sigma w(|F_o| - |F_c|)^2$, where $w = [2F_o/\sigma - (F_o^2)]^2$ and $\sigma(F_o^2) = [\sigma^2(I) + \rho^2 I^2]^{1/2}$ with ρ assigned a value of 0.01. Expressions for the residuals are $R = \Sigma||F_o| - |F_c||/|F_o|$ and R_w $[\Sigma w(|F_o - F_c|)^2/\Sigma w(F_o^2)]^{1/2}$.

(40) (a) Ammeter, J. H.; Burgi, H.-B.; Thibault, J. C.; Hoffmann, R. *J. Am. Chem. Soc.* **1978**, *100*, 3686. (b) Hoffmann, R. ICON8, QCPE no. 344.